



YAŞAR UNIVERSITY
GRADUATE SCHOOL OF NATURAL AND APPLIED SCIENCES

MASTER THESIS

**GPR RAW-DATA ANALYSIS TO DETECT CRACK VIA
WAVELETS AND DEEP LEARNING METHODS**

MUSA BINDAWA TANIMU

THESIS ADVISOR: ASST.PROF.DR. NALAN ÖZKURT

CO-ADVISOR: ASSOC.PROF.DR. GÖKHAN KILIÇ

ELECTRICAL AND ELECTRONICS ENGINEERING

PRESENTATION DATE: 11.06.2019

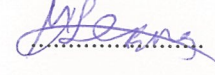
BORNOVA / İZMİR
JUNE 2019

We certify that, as the jury, we have read this thesis and that in our opinion it is fully adequate, in scope and in quality, as a thesis for the degree of Master of Science.

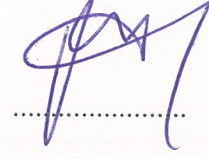
Jury Members:

Prof.Dr. Mustafa Seçmen
Yaşar University

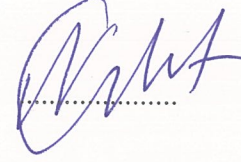
Signature:



Asst.Prof.Dr. Özgür Tamer
Dokuz Eylül University



Asst.Prof.Dr. Nalan Özkurt
Yaşar University



Prof.Dr. Cüneyt Güzeliş

Director of the Graduate School

ABSTRACT

GPR RAW-DATA ANALYSIS TO DETECT CRACK VIA WAVELETS AND DEEP LEARNING METHODS

Tanimu, Musa Bindawa

Msc, Electrical and Electronics Engineering

Advisor: Asst.Prof.Dr. Nalan Özkurt

Co-Advisor: Assoc.Prof.Dr. Gökhan Kılıç

JUNE 2019

This thesis is about detecting cracks on infrastructures such as roads and bridges which may result in several problems in future. There are several methods for detecting cracks which can be summarized as destructive and nondestructive. This study aims to analyze cracks in materials by using non-destructive techniques (NDT) especially Ground Penetrating Radar (GPR) analysis because of its many advantages over other NDTs as will be seen under the literature review.

In this study, a laboratory environment is constructed and GPR and thermal image measurements of several cracked and non-cracked slabs of different shapes and materials were conducted. Then after visual and thermal analysis, the GPR raw-data is analyzed with wavelet transform and entropy analysis. Finally, the continuous wavelet transform coefficients are classified with deep learning methods, specifically convolutional neural network and the classification accuracy was calculated.

Furthermore, a case study of a bridge used for previous research works was used to test the methods on a larger scale. The results show that the Wavelet-CNN crack detection method proposed is better than detecting cracks directly from the raw-data or b-scan signals.

ÖZ

YER RADARI HAM VERİSİ ANALİZİ İLE KIRIKLARIN DALGACIK VE DERİN ÖĞRENME YÖNTEMLERİ İLE TESPİTİ

Tanimu, Musa Bindawa

Yüksek Lisans

Danışman: Dr.Öğr.Üyesi Nalan Özkurt

Yardımcı Danışman: Doç.Dr.Gökhan Kılıç

Haziran 2019

Bu tez, yollar ve köprüler gibi altyapılarda gelecekte sorunlara yol açabilecek çatlakların tespit edilmesi ile ilgilidir. Çatlakları tespit etme yöntemleri tahribatlı ve tahribatsız olarak iki grupta incelenir. Bu çalışma tahribatsız yöntemleri özellikle de diğer yöntemlere kıyasla birçok avantajı nedeniyle yer radarı analizleri kullanarak materyallerdeki çatlakları analiz etmeyi amaçlamaktadır.

Bu çalışmada, bir laboratuvar ortamı oluşturulmuş ve farklı şekil ve malzemelerde kırıklı ve kıriksiz çeşitli blokların yer radarı ve termal görüntü ölçümleri yapılmıştır. Sonra görsel ve termal analizin ardından, GPR ham verileri dalgacık dönüşümü ve entropi yöntemleri ile analiz edilmiştir. Son olarak, sürekli dalgacık dönüşümü katsayıları derin öğrenme yöntemleriyle, özellikle evrimsel sinir ağı ile sınıflandırılmış ve sınıflandırma doğruluğu hesaplanmıştır.

Ayrıca, önceki araştırma çalışmaları için kullanılan bir köprüye ait bir vaka çalışması, yöntemleri daha geniş bir ölçekte test etmek için kullanılmıştır. Sonuçlar, önerilen Wavelet-CNN çatlak tespit yönteminin, ham veri veya b-tarama sinyallerinden doğrudan çatlakları tespit etmekten daha iyi olduğunu göstermektedir.

ACKNOWLEDGEMENTS

This has been the most difficult year of my life, working on this thesis and battling anxiety. I would like to thank God for this opportunity. I would also like to give thanks to my two super supervisors Asst.Prof.Dr. Nalan Özkurt and Asst.Prof.Dr. Gökhan Kılıç for providing me with the support I needed and for always welcoming me with open arms even at inconvenient hours. To my north-star, friends and family, I can't begin to explain how much your love and support has meant to me throughout this journey.

This thesis has opened my mind and taken me on a journey of discovering new and vital information which is helpful to my growth and development in my career path and as a person.

I can't thank you all enough.

Musa Bindawa Tanimu


İzmir, 2019

TEXT OF OATH

I declare and honestly confirm that my study, titled GPR RAW-DATA ANALYSIS TO DETECT CRACK VIA WAVELETS AND DEEP LEARNING METHODS and presented as a Master's Thesis, has been written without applying to any assistance inconsistent with scientific ethics and traditions. I declare, to the best of my knowledge and belief, that all content and ideas drawn directly or indirectly from external sources are indicated in the text and listed in the list of references.

Musa Bindawa Tanimu

Signature



.....

June 11, 2019

TABLE OF CONTENTS

ABSTRACT	iii
ÖZ	iv
ACKNOWLEDGEMENTS	v
TEXT OF OATH.....	vi
Table of contents	vii
LIST OF FIGURES	ix
SYMBOLS AND ABBREVIATIONS.....	x
CHAPTER 1 INTRODUCTION	1
1.Motivation of research	1
2.Aims and objectives of the study	2
3.Layout of the thesis	3
CHAPTER 2 Literature Review and Background Studies	4
1.NON-DESTRUCTIVE METHODS	4
2.INFRARED THERMOGRAPHY(IT).....	4
3.ULTRASONIC TESTING	5
4.IMPACT ECHO (IE).....	5
5.GAMMA RAY RADIOGRAPHY	5
6.THERMAL CAMERA.....	6
7.3D-LASER SCANNER	8
8.GROUND PENETRATING RADAR (GPR).....	9
(1) Working principle.....	10
(2) Transmitter antennas	12
(3) Receiver antennas.....	12
(4) Antenna types.....	13
A. Dipole antenna	13
B. Broadband dipole antenna	13
C. Bow-tie dipole antenna.....	13
(5) Attenuation.....	14
(6) Scattering.....	14
(7) Dielectric Permittivity.....	14
(8) Relative Permittivity	14
(9) Propagation Velocity	15
(10) GPR APPLICATIONS	15
SUMMARY.....	18
CHAPTER 3 METHODOLOGY	19

1.SIGNAL PROCESSING.....	19
2.WAVELETS	19
(1) WAVELET TRANSFORM.....	21
(2) WAVELET ESSENTIALS.....	24
(3) COMPLEX WAVELETS	24
(4) ENTROPY	26
3.NEURAL NETWORKS	27
4.CONVOLUTIONAL NEURAL NETWORKS.....	30
CHAPTER 4 EXPERIMENTS AND RESULTS	32
1.EXPERIMENTAL SETUP	32
(1) VISUAL INSPECTION.....	33
(2) THERMAL CAMERA.....	34
(3) GROUND PENETRATING RADAR.....	35
2.RESULTS AND ANALYSIS.....	37
(1) VISUAL ANALYSIS OF RAW-DATA.....	37
(2) VISUAL ANALYSIS OF SIGNALS.....	43
(3) THERMAL IMAGE ANALYSIS	44
(4) WAVELET ANALYSIS OF SIGNALS	46
(5) ENTROPY ANALYSIS.....	48
3.CNN CLASSIFICATION	50
4.CASE STUDY	52
CHAPTER 5 CONCLUSION AND FUTURE WORK	57
REFERENCES.....	59
APPENDIX 1 – CWT with Matlab.....	62
APPENDIX 3 – Training CNN to classify new image.....	64
APPENDIX 4 – Single-Level 2-D Discrete Wavelet Transform of an Image with Matlab....	66
APPENDIX 5 – Resizing image to 224.....	67

LIST OF FIGURES

Figure 1.1. Schematics of approach	3
Figure 2.1. The basic principle of GPR	11
Figure 2.2. Relationship between A-scan, B-scan and C-scan	11
Figure 2.3. Example of A-Scan	11
Figure 2.4. Example of B-Scan	12
Figure 3.1. A Morlet wavelet	24
Figure 4.1. Experimental Setup	31
Figure 4.2. Cracking a slab	32
Figure 4.3. Thermal Camera	33
Figure 4.4. Thermal camera images	34
Figure 4.5. GPR Device	34
Figure 4.6. Taking GPR Reading	35
Figure 4.7. Concrete slab with 1cm crack, B-scan and average trace spectrum	35
Figure 4.8. Concrete slab with 2cm crack, B-scan and average trace spectrum	37
Figure 4.9. Cylindrical concrete slab with no crack, B-scan and average trace spectrum	38
Figure 4.10. Cracked cylindrical concrete slab, B-scan and average trace spectrum	39
Figure 4.11. Wooden slab, average trace spectrum and B-Scan	40
Figure 4.12. Solid cubic concrete slab, B-scan and average trace spectrum	41
Figure 4.13. Plot of all signals	42
Figure 4.14. CNN classification results	46
Figure 4.15. Classification accuracy	48
Figure 4.16. The pentagon bridge	49
Figure 4.17. Vertical slices of bridge data(left), Computer model of position of anomalies(middle), real life location of anomalies(right)	49
Figure 4.17. Thermal camera images	50
Figure 4.18. Thermal camera images	55

SYMBOLS AND ABBREVIATIONS

ABBREVIATIONS:

NDT Non-destructive testing

GPR Ground penetrating radar

IT Infrared thermography

IE Impact echo

CNN Convolutional neural networks

NN Neural network

SVM Support vector machine

SYMBOLS:

α Attenuation constant

ϵ Permittivity

ψ Wavelet function

\vec{E} Electric field

CHAPTER 1

INTRODUCTION

1. Motivation of research

Bridges, tunnels, roads, etc. play a significant role in our lives and society. We need them for our daily activities and connection to the rest of the world. These structures are of crucial importance. However, a lot of these structures are not in good condition because they were built a long time ago. It is common for old structures to encounter structural defects such as cracks, delamination, and moisture absorption, which all can weaken structures and, in severe cases, to lead to their ultimate failure. The failure of these structures has led to damage of properties and even loss of lives in severe cases. A recent example is the collapse of the Genoa bridge in Italy, which claimed the lives of over 43 people. These problems call for the urgent need for health analysis of these structures and the repair/rebuilding of damaged ones. The health of these structures should be checked, keeping in mind that properties & the lives of humans are at stake.

Nigeria is shutting down its busiest bridge for 27 months to perform inspection and maintenance. These inspections are only taking this long due to the extensive reliance and use of old/traditional destructive techniques. Nonetheless, waste of time and obstruction of busy traffic like this can be avoided by using existing efficient techniques, and developing new techniques. Many roads and other structures in Nigeria fail due to the lack of proper health checking techniques. The structural defects such as; cracks, sinkholes, etc. are only discovered when it's too late.

Modern developments in non-destructive testing (NDT) methods saves time and reduces maintenance costs. These techniques such as GPR, Thermal camera imaging, Infrared thermography, etc., are useful in avoiding wasteful spending in repairs and in giving structures a better chance to reach their full lifespan which prevents potential loss of lives in the case of the structures failing.

It is now possible to check the health status of structures using these non-destructive methods. As the name implies, these methods do not cause any physical damage to structures. They are time efficient and provide important information to engineers for

finding and assessing features in structures. The methods are cheap and can be used for long-term structural health evaluation.

As technology develops, new non-destructive techniques emerge, and old ones are improved. Different NDTs are used for various applications depending on the pros and cons.

GPR is widely used for various applications because it saves time; it is easy to use; it is inexpensive compared to other methods, etc. However, GPR data is sometimes hard to understand because of noise and scattering.

Roads, bridges, pavements and other concrete structures crack as time passes due to overloading, improper drainage, weather factors, lack of proper design/maintenance, etc. These cracks lead to the poor performance of the roads, affecting traffic flow and in some unfortunate situations, accidents

2.Aims and objectives of the study

As will be viewed under the literature review, in the course of this thesis, various techniques will be discussed emphasizing GPR and comparing its results with that of Thermal Camera. The goal of this thesis is to analyze GPR raw-data to detect crack via wavelets and machine learning methods. To achieve this goal the following objectives were set:

1. To do the necessary research on various NDTs and make sure that GPR is the most appropriate
2. To learn how to operate the GPR and thermal camera, collection, and processing of GPR data.
3. To set up the laboratory for the experiment.
4. To do the necessary research for gaining knowledge on the methodology
5. To bring together the knowledge gained to do the required analysis.

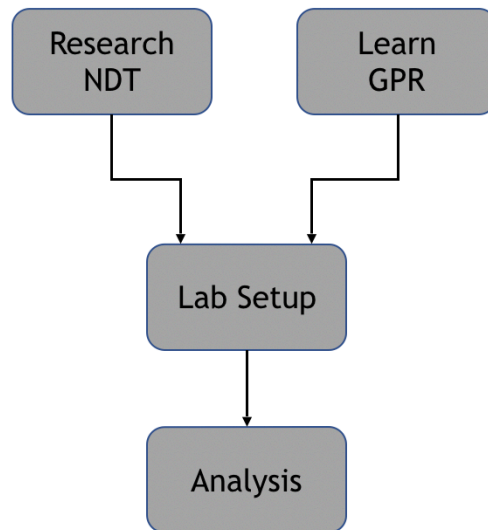


FIG 1.1. Schematics of approach

3. Layout of the thesis

This thesis contains an abstract, acknowledgments, text of oath, appendix, and the following chapters:

1. Chapter 1: INTRODUCTION: This chapter introduces readers to the thesis. It contains the background study, aim, and objective of the thesis.
2. Chapter 2: LITERATURE REVIEW: This chapter includes literature concerning structural health assessment and non-destructive techniques. It talks about various NDTs with their pros and cons with emphasis laid on GPR. It also gives an insight on the methods used in the thesis.
3. Chapter 3: METHODOLOGY: This chapter discusses wavelets, neural networks, and convolutional neural networks, which are the methods used in this thesis.
4. Chapter 4: EXPERIMENTS AND RESULTS: This chapter contains the experimental setup and the results collected from these experiments.
5. Chapter 5: CONCLUSIONS: This chapter summarizes the objectives and results of the thesis. Pathways to future improvement is also presented in this chapter.

CHAPTER 2

LITERATURE REVIEW AND BACKGROUND STUDIES

Non-Destructive Testing methods are vital in structural health assessment. They save time, reduce costs, and do not cause physical damage to the structures.

As technology develops, new non-destructive techniques emerge, and old ones are improved. Various NDTs are used for different applications depending on the pros and cons. In the course of this thesis, numerous techniques will be discussed, but emphasis will be laid on GPR and comparing its results to that of Thermal Camera.

GPR is a commonly used technique because it is time-saving, easy to use, and it is cheap compared to other methods. However, it has its disadvantages. Its data is sometimes difficult to comprehend because of noise and scattering.

Roads, bridges, pavements and other concrete structures crack as time passes due to overloading, improper drainage, weather factors, lack of proper design/maintenance, etc. These cracks lead to the poor performance of roads, affecting traffic flow and in some unfortunate situations, accidents.

1. NON-DESTRUCTIVE METHODS

As mentioned earlier, NDTs do no physical damage to structures. They also ensure structural quality. Therefore, NDTs are the most preferred assessment methods used. They provide information on structural defects and structures' composition while causing no physical damage because no removal of samples from the structures is required (Shreedhar,2017) (Kilic,2016).

As technology advances, new NDT techniques emerge. For example, gamma ray radiography, ultrasonic testing, infrared thermography, impact echo, GPR, etc.

2. INFRARED THERMOGRAPHY(IT)

This is a non-destructive assessment method that needs to make some surface contact to gain internal information. It detects the different spectral characteristics of infrared energy emitted from the structures with an infrared camera, providing the results in the form of a color-coded image. It can detect non-uniformities, inclusions, delamination, debonding, and cracks. This method is often used for the location of flaws and defects in civil engineering structures. It has also been successfully employed in other fields like medicine, printing, and in identifying hidden mine-

shafts. It is commonly used to evaluate the health of concrete bridge decks. IT is a method of reasonable cost and is capable of detecting surface and internal defects. The method is portable. Therefore, it enables an assessment to be carried out without interrupting traffic. IT poses some disadvantages. Its results are affected by various weather conditions, and it requires a skilled operator to control the system (Kilic, 2016).

3. ULTRASONIC TESTING

This is a non-destructive assessment method that is used for locating existing defects, rods, and pipes. It is relatively cheap. It is also used to measure concrete's modulus of elasticity. Before the inspection process, the test surface must be ground smooth and be cleaned. This method uses frequency sound waves ranging from 1 to 10 MHz, and the wave types are classified depending on the mode of vibration of the medium, which can be longitudinal, transverse, and surface waves. This method needs a skilled operator, and its application of structural assessment is limited (Kilic,2014) (Kilic,2016).

4. IMPACT ECHO (IE)

This is a non-destructive assessment method of detecting defects in concrete by sending a quick mechanical impact on a sample and then analyzing the stress waves which the impact has caused to travel through the sample. These stress waves send back information which is recorded upon contact with border points in cases of delamination, voids, cracks, large steel bars, and with any boundary edge. This method is relatively low/medium cost. Its disadvantage includes the reduction of signal due to material deformation. When the sample is struck, the receiver is not very sensitive, and the scattering that occurs due to heterogenous characteristics of concrete can interfere with the returning signal at boundaries, noise within the data is common. A skilled operator is needed because the method is not as straightforward as other NDTs (Kilic,2014) (Kilic,2016).

5.GAMMA RAY RADIOGRAPHY

This method uses the gamma ray techniques of radiography and radiometry. Small quantities of gamma radiation created by a decaying radioisotope are applied to the concrete to be tested. Some of this radiation travels directly through the sample, some of it is absorbed, and the presence of electrons in the concrete causes the

radiation to be scattered. The pattern of this scatter gives information on the properties of sub-surface materials. This method is vital in identifying the size, position, and quality of reinforcement, moreover, it is essential in detecting voids in concrete and the difference in compression. The equipment is lightweight and does not require external power.

Disadvantages of this method include; being relatively expensive, the need for accessibility to both sides of the sample, its limited capacity, time consumption in developing images, existing strict safe guidelines attached to its use, its inability to be switched off, and the fluctuating strength of the isotope (Kilic,2014) (Kilic,2016).

6.THERMAL CAMERA

The differences between objects that are enlightened by the sun or other sources of light can be seen by human eyes. Thermal cameras can detect heat energy off objects. Every object has heat energy that infrared cameras use to detect images. Because of this, thermal infrared cameras function even in pitch darkness.

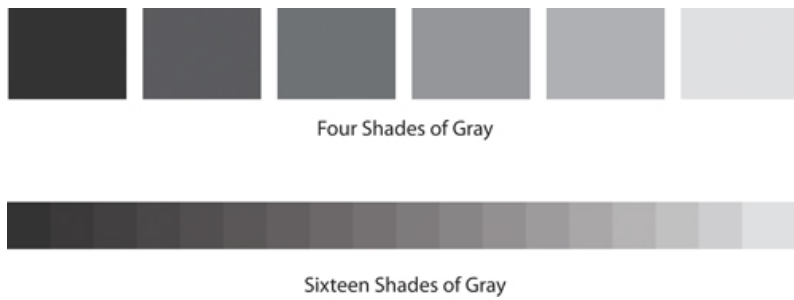
Thermal images are not like typical camera images or images seen by our naked eyes. Thermal cameras are configured to change the temperature of images into tones of grey, which are brighter or darker than the background to show the heat in a format for human eyes. If the weather is cold, a person is warmer than the background, so they appear brighter. On a hot day, a person appears darker because they are cooler than the background.

At night, the background temperature is cooler than 98.6 degrees, which is the temperature of a person; this is why the thermal cameras see in the dark. Under favorable conditions, people are easily detected at night because they appear brighter than the background even in pitch darkness.

However, conditions are not always favorable. During the day, objects might take up heat energy from the sun and get hotter. This is known as thermal loading. When all the objects have almost the same temperature, the cameras face difficulty because the temperature difference leaves them with a narrow presentation range. The resulting images end up being whited out, greyed out or undefined.

Thermal cameras can display the 16,384 shades of gray in 250 gray scales, which is more fitting for the human eye to interpret.

Below is an image which shows how difficult it is to differentiate the various shades of gray. At the top are six shades which the eyes plainly see. At the bottom, we have sixteen shades which are harder to differentiate between neighboring shades. The thermal camera has over 16,000 shades of gray, which is over 1,000 more than in the image below. This shows how big the problem is.



Modern Thermal cameras have colorization functions. Objects having temperatures above the threshold temperature are shown in bright colors. The locations of objects with high temperature are easily detected even in challenging conditions because of the bright colors.

Cold spots are easily detected due to the colorization function. The cold spots are examined by setting a low threshold temperature. The colorization function is significant in detecting gas leaks, water lines, heat elopement positions, patency of breathing apparatus, etc. (Szajewska, 2017).



Thermal imaging is used in detecting sinkholes. Sinkhole disasters are increasingly happening and need to be evaluated. Sinkholes can be tested by drilling and cone penetrometer test. However, these destructive techniques can worsen the sinkhole,

and have less chance of detecting them. GPR, seismic waves, electric resistivity tomography, GB-InSAR, and other non-destructive techniques can be used but they have limited applications and most of them are manual. A combination of CNN and Thermal camera mounted on a drone can be used to detect sinkholes at a broader area at a cheap cost (Lee,2016).

Fire fighters use Thermal cameras. It can be used in fighting building fires. Moreover, it can be used in finding lost people and animals in darkness or fog. It can also be used to combat other effects of a natural disaster. Thermal cameras are small and easy to use. The heated objects are easy to spot even in difficult conditions because they are shown with bright colors. Spotting the hotter regions in a fire and information on the regions make it easier to handle the fire. Victims of fire outbreaks are reached faster and more safely because of thermal cameras (Szajewska, 2017).

7.3D-LASER SCANNER

This is an NDT that digitally captures the structures of objects using a laser beam without contact. This is a way of capturing the actual shape and size of an object by forming point clouds of data from the exterior of the object and representing in digitally in 3D.

3D-laser scanning is the best method of inspecting contoured surfaces and complicated shapes that need large data to be accurately represented.

The object that will be scanned is placed at the bottom of the digitizer. Special software guides the laser probe over the object. The laser probe reflects a light laser beam on the object while two sensor cameras record the change in distance and shape of the laser beam in 3D(XYZ) as it moves along the object.

The shapes of the object are shown on the computer as millions of points known as “point clouds” captures the shape of the object as a laser

After the large point cloud data is formed, it is registered and combined into a 3D representation of the object and processed with different software for different applications.

The 3D-Laser Scanner’s biggest advantage is its measurement accuracy, which can be improved (Isa,2017).

8.GROUND PENETRATING RADAR (GPR)

This non-destructive method is used to detect underground objects and predict their depths. These objects are cables, pipes, and landmines or any other dielectric material. Objects like unexploded ordnance (UXO) have been detected using GPR in both civilian and military fields for many years. It is also used for the detection of anti-tank and anti-personnel mines. GPR has been widely used to carry out archeological investigations to identify buried targets with improved horizontal and vertical resolution compared to other geophysical methods (Smitha,2017) (Ghozzi, 2017) (Thakur,2016) (Kobashigawa,2011).

GPR technology is a highly considered assessment method used by both scientists and engineers because of its advancement in recent years. Apart from engineers and scientists, professionals and practitioners from archaeology, geology, geotechnics, glaciology, forensics, and hydrology have all found uses for GPR in diverse ways in their various fields. The system uses radio-wave energy to locate and identify sub-surface features such as pipes, foundations, land mines, and geological layers (Kilic, 2016).

GPR is the go-to method for Non-Destructive Testing (NDT) in civil engineering. The GPR method is used for assessment and monitoring of civil engineering structures due to its detailed data production on the present state of structures, allowing detection of potential areas of damage. Ground penetrating radar (GPR) systems use an antenna to transmit electromagnetic waves into a structure to evaluate and detect the structure's health by using the collected data of different kinds of civil structures (Shreedhar,2017) (Kilic,2016) (Kilic,2018).

GPR is a non-destructive method that detects underground and invisible media efficiently, thereby achieving visualized results. It is widely used in nondestructive bridge, road, pipe, and tunnel measurements (Wang,2018).

It has high data acquisition rate, and it is sensitive to the differences of permittivity, water content. It can be used to carry out archeological investigations without excavation. GPR is gaining popularity in tunnel evaluation because it is a comparatively cheaper method (Shreedhar,2017) (Thakur,2016) (Kilic,2018).

(1) Working principle

GPR is a high-resolution electromagnetic method. An electromagnetic wave which is radiated from a transmitting antenna which travels through a material at a velocity which is dependent on the permittivity of the material. This wave spreads out and descends until it is obstructed by an object with a different electrical property from the material that surrounds it. The wave bounces off the object and scatters upwards and is detected by a receiving antenna.

This method can explore the depth of a few meters and a resolution of a few centimeters by transmitting and receiving electromagnetic waves (Wang,2018) (Pasolli,2008).

The frequency and attenuation of the reflected wave are proportional to the travel depth. The attenuation of different frequency varies at every interval. The higher the frequency, the higher the attenuation. The detection of objects underground by the GPR is dependent on the electromagnetic properties of the medium being penetrated (Yao,2007) (Kilic,2018).

The location of the underground features is determined by the total travel time of the reflected and received waves and the velocity of the GPR waves. The total travel time of the reflected and received waves is gotten from the GPR profiles, and the velocity of the waves depends on the dielectric constant of the medium.

A 1D signal is gotten after placing an antenna above a specific position. It is called an A-Scan (FIG 2.3). GPR signals are non-stationary signals in a dispersive medium, and are attenuated by scattering, absorption, etc. The waves from the transmitting antenna travel through the ground hitting the buried objects and then are reflected to the receiver (FIG 2.1) to form an A-scan. Different A-scans at different scan positions are combined to form a B-scan (FIG 2.4) GPR image. Furthermore, combining 2D B-scans form to be a 3D C-scan (FIG 2.2) (Ghozzi,2017) (Almaimani, 2018).

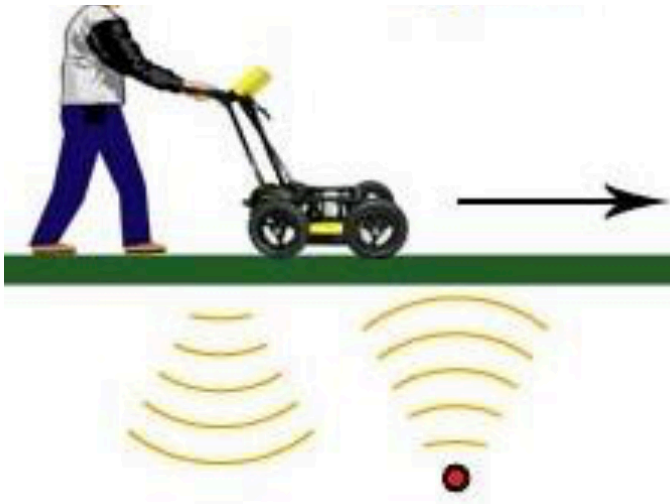


FIG 2.1. The basic principle of GPR

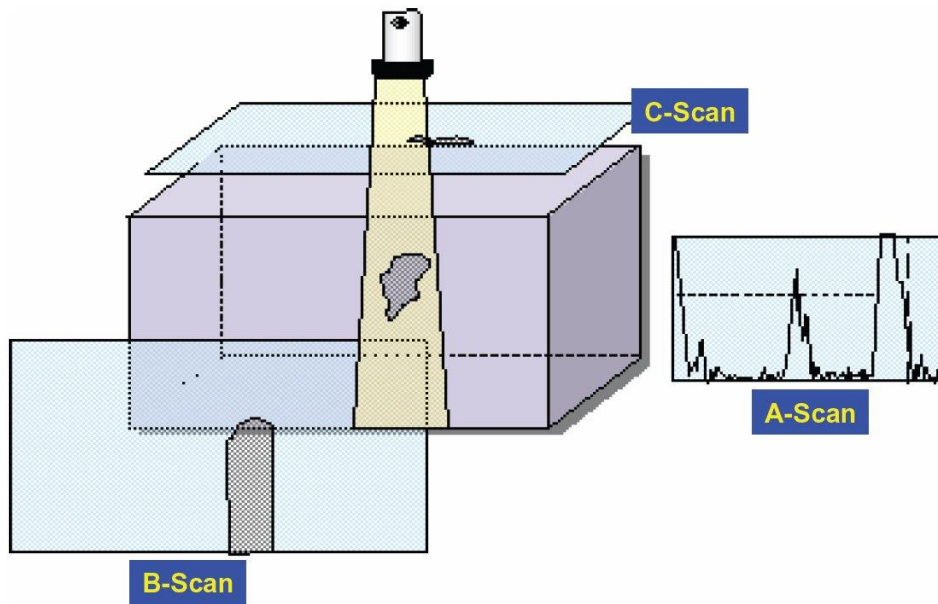


FIG 2.2. Relationship between A-scan, B-scan, and C-scan.

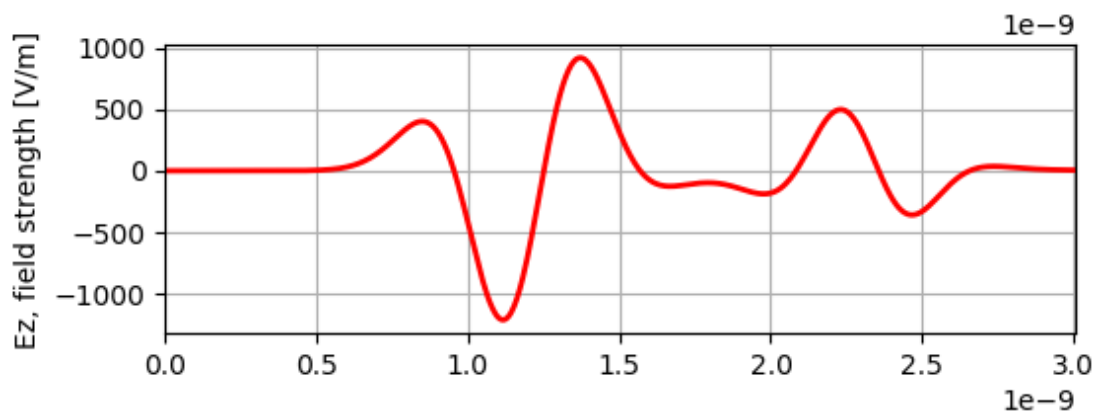


FIG 2.3. Example of A-Scan

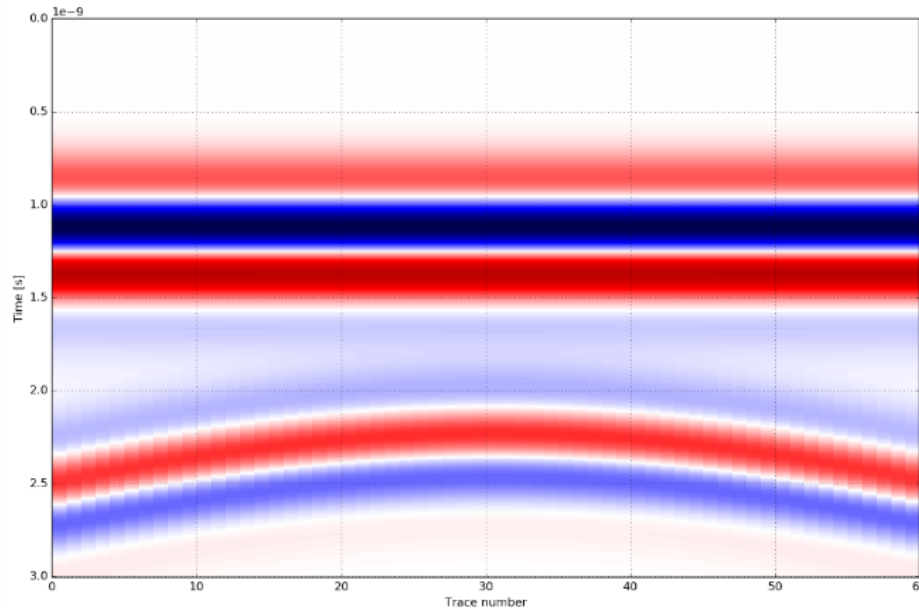


FIG 2.4. Example of B-scan

High Frequency GPR is used in highway quality testing, tunnel detection, and airport runway detection because of precision. Low frequency GPR has better penetration depth. The higher frequency antenna can detect objects of smaller dimensions at shallow depths, whereas a low frequency antenna transmits waves to a greater depth by compromising the capacity or resolution. High frequency is used for applications that need better resolution, and low frequency is used for applications that need more penetration depth (Thakur,2016) (Kilic,2018) (Almaimani,2018).

(2) Transmitter antennas

GPR transmitter antennas have an open circuit which carries a wavelet. The current carried within the antenna generates a pulse of radio-waves, which is also a wavelet signal. GPR transmitter antennas generate a signal with very high frequency content. The characteristics of the GPR signal depends on the wavelet, its frequency content, and the shape of the transmitter antenna (GeoSci,2015).

(3) Receiver antennas

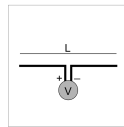
The receiver antenna makes GPR measurements. Transmitter antennas convert electrical current into radio-wave signals, which makes them transducers. Receiver antennas are also transducers, which convert radio-wave signals to electrical current. GPR receiver antennas are designed to measure radio-wave signals generated by the transmitter antenna correctly. GPR systems are designed to use near-identical antennas for the transmitter and receiver (GeoSci,2015).

(4) Antenna types

There are different transmitter antennas used for GPR. The frequently used ones are listed below.

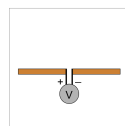
A. Dipole antenna

These consist of two bilateral conductive rods. The efficiency of these depend on their length. GPR Dipole Antennas are designed to have a length which works well for a particular operating frequency. They typically have lengths of 10s of centimeters up to a few meters (GeoSci,2015).



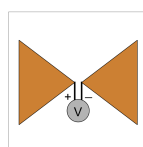
B. Broadband dipole antenna

These are made from dipole antennas by increasing the width of the conductive rods or using elongated conductive plates. More effective transmission of frequency contents of the source wavelet signal can be achieved by making the antennas sufficiently broadband. This antenna type is best used for operating frequencies below 250 MHz (GeoSci,2015).



C. Bow-tie dipole antenna

Bow-tie antennas consist of two symmetrically oriented flat conductors. Bow-tie dipole antennas are designed for operation at frequencies between 100 MHz and 1 GHz. Bow-tie transmitters transmit signals with larger bandwidths more effectively compared to dipole antennas. They are superior when transmitting short wavelength high frequency radio-wave signals. This antenna typically has dimensions on the order of 10s of centimeters; which makes them more compact than the broadband dipole antennas used for GPR (GeoSci,2015).



(5) Attenuation

This is the constant loss in the amplitude of a wave as it travels through a medium. The rate of loss in amplitude is known as attenuation constant (α). For an electromagnetic wave with distance traveled, the attenuation constant is:

$$\frac{|A|}{|A_0|} = e^{-\alpha z}$$

Given is the wave's initial amplitude and is the wave's amplitude after traveling a distance. So $z \rightarrow \infty$, the wave's amplitude goes to zero. Furthermore, for bigger values of the wave attenuates faster.

(6) Scattering

- Scattering occurs when electromagnetic waves change paths because of non-uniformities; which are less than 1/4 the wavelength of the radio-wave signal. Scattering is not good for GPR because it reduces the amplitudes of useful signals and increases unwanted noise. Causes of scattering are:
 - Non-uniform surface shape of bigger buried objects.
 - Rocky soils, which highly contributes to the scattering of GPR signals.
 - Clutter made up of small buried objects.

(7) Dielectric Permittivity

Dielectric permittivity (ϵ) is an important physical property for ground penetrating radar. This physical property affects the wavelength, velocity, and attenuation of electromagnetic waves as they travel through a material. It is the ratio of the electric field (E^{\rightarrow}) within a material and the corresponding electric displacement (D^{\rightarrow}):

$$\vec{D} = \epsilon \vec{E}$$

(8) Relative Permittivity

The dielectric properties of materials are commonly indicated using the relative permittivity (ϵ_r). The relative permittivity interprets the dielectric properties of a material relative to that of free-space:

$$\epsilon_r = \frac{\epsilon}{\epsilon_0}$$

(9) Propagation Velocity

Radiowaves have different travel speeds for different materials. The arrival times of GPR signals are directly affected by the propagation velocity of the Earth. Radio-waves velocity is dependent on the physical properties of the medium. The velocity of radio-waves through a homogeneous material is:

$$V = \sqrt{\frac{2}{\mu\epsilon} \left[\left(1 + \left(\frac{\sigma}{\omega\epsilon} \right)^2 \right)^{1/2} + 1 \right]^{-1/2}}$$

The approximate dielectric permittivities, electrical conductivities, and radio-wave velocities for different materials are given below.

- N.B; the unit for electrical conductivity is milli-Siemens per meter
- N.B; the velocity is in meters per nanosecond. For conversion to m/s, simply multiply by 10^{-9}

Material	Relative Permittivity	Conductivity (mS/m)	Average Velocity (m/ns)
Air	1	0	0.3
Fresh Water	80	0.5	0.033
Sea Water	80	3000	0.01
Ice	3-4	0.01	0.16
Dry Sand	3-5	0.01	0.15
Saturated Sand	20-30	0.1-1	0.06
Limestone	4-8	0.5-2	0.12
Shales	5-15	1-100	0.09
Silts	5-30	1-100	0.07
Clays	5-40	2-1000	0.06
Granite	4-6	0.01-1	0.13
Anhydrites	3-4	0.01-1	0.13

The velocity and attenuation of the waves transmitted from GPR depend largely on the conductivity and dielectric properties of the assessed medium (Kilic,2014).

(10) GPR APPLICATIONS

GPR has a broad range of applications in different fields. It is used for checking structural health of bridges, roads, tunnels, etc. It is also used for detecting defects in materials like concretes. Additionally, it is used in the research of historical structures. Below, are examples of GPR applications.

A GPR survey was conducted at the ancient Greek city of Notion in June 2017 to explore possible buried roads and houses, to map and identify their depths. The site

is located at Menderes in the south of Izmir. Notion has been a site of various archeological research for the past 100 years. Other non-invasive techniques such as aerial and thermal imagine, visual inspection, near-surface geophysical prospection, etc. have been previously used but these techniques did not provide depth estimates of the identified features and masked some details of these features. The GPR survey complimented all the prior work with better resolution and depth estimates, which provide a clearer plan of the structures. It provided meaningful results which will be very helpful for future investigations (Yigit,2017).

GPR investigations were carried out at some archeological sites in Vadnagar, India. This city's known history goes back to 2300 BC. The archeological potential of this city deems it necessary for explorations to understand the process of evolution of society. The results of the investigation indicated the presence of metallic objects/ high mineral soil lumps beneath the ground. The potential presence of ash layers was detected in some areas. The presence of wall-like structures was also observed. These results can be used to plan further excavation (Thakur,2016).

GPR has been used for evaluation of structural integrity of roadways because it has advantages over other NDTs and destructive techniques. Pavement defects are classified as open and embedded defects. Open defects are visible and detectable with a visual inspection. Embedded defects can be detected using GPR. It helps determine the thickness of layers and detects cracks within pavements with the help of SVM, which makes it helpful in the maintenance of roads (Shreedar,2017).

Combining GPR with advanced processing and presentation methods played a vital role in the tunnel boring project at a dam and hydro-power station. Tunnels are essential in many infrastructures such as roadways, sewer systems, railway lines, etc. GPR has been used to locate rebar, check second lining thickness, check for existing karst conduit or important rock features under tunnels. Tunnel excavation process is vulnerable to the existence of karst conduits and voids; it is crucial to detect these underground systems. Some defects were found after the tunnel was inspected visually. The GPR method showed potential in modeling the structures' future health. It also showed the existence of karst conduits in the pathway of the tunnel project, buried pipes, etc. This study shows the success of GPR technology in highlighting

the hidden features, thereby potentially preventing expensive errors in the tunneling process. This system is potentially widely applicable. (Kilic,2018)

A case study was done on a bridge using GPR to learn the health of the bridge and to locate rebar, moisture and other features. New computer technology and improved Neural networks have had a significant impact on bridge health assessment using GPR. The negative effect of moisture presence was identified using GPR in this case study. The radiograms showed an abnormality in the position of rebars due to the presence of moisture (Kilic,2014).

SUMMARY

Non-Destructive Techniques are essential because they save time and money. Most of the NDTs need little or no structural contact to perform analysis. Therefore, they do not damage structures. As technology develops, there is a greater variety of NDTs to choose from each having their advantages and disadvantages. GPR is currently the most used due to its advantages over the other methods.

The human eye has an exceptional focusing ability and can be competent in identifying particular features, differentiating between colors, and can detect discontinuities, size, shape, depth, brightness contrast, and texture. As a result, visual inspection remains valuable within the field of structural assessment. Regular visual inspection by trained personnel can detect defects at an early stage to prevent obstruction of operation of a structure. The traditional structural assessment method of visual inspection is still in use today even though it is only useful in terms of identifying flaws visible on the surface of a structure, and is open to mistakes because it relies on humans who make judgment errors. The information gained from this type of inspection is only on the surface, vulnerable to error, provides only qualitative data, and is inadequate (Kilic,2016).

Humans are bound to make mistakes leading to unstable classifications due to tiredness, forgetfulness, and complexity of features. Computerized methods have been developed to avoid this. The combination of NNs and NDTs leave little margin for error and saves a lot of time.

CHAPTER 3

METHODOLOGY

1.SIGNAL PROCESSING

Signals are processed for noise removal to get the information needed from them fully.

GPR signals have frequency, amplitude, and phase, among other features. These features show the characteristics of the transmitted and received signals, which point out the underground target. Target recognition and signal detection are mattering points in GPR data processing. Wavelet transform and other signal processing techniques help us get important components of the signals (Wei,2010).

The detection of peak (values and positions) is an important step in most signal processing applications. Threshold methods, Hilbert transformation, wavelet transformation, the combination of Hilbert and wavelet transformation, fuzzy c-means clustering, k-means clustering, etc. are examples of peak detection techniques (Ghozzi,2017).

2.WAVELETS

Wavelets are mathematical functions which separate data into various frequency components. They join every component with a resolution with similar scaling and then studies each component. For signals with sharp spikes and disruptions, wavelets have advantages over other Fourier analysis methods. Wavelets have various applications in signal processing, image compression, etc. (Addison,2017).

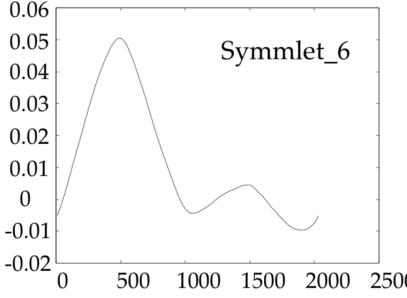
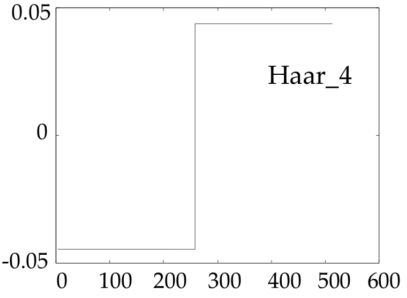
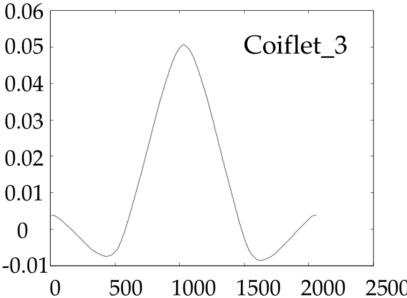
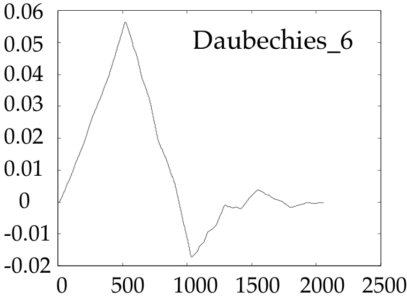
The main idea behind wavelets is the analysis of data according to scales. Wavelet algorithms analyze data at different resolutions and scales. The Mother wavelet is the default function used in wavelet analysis. Depending on the data components, the mother wavelet is expanded, contracted, or scaled to match the resolution.

Similar to Fourier analysis, wavelet analysis works by expanding functions concerning a group of basis functions, but unlike Fourier analysis, wavelet analysis expands the functions with wavelets and not with sines and cosines. Wavelets come in handy in the processing of non-stationary signals.

Discrete Wavelet Transform is similar to Fast Fourier Transform.

There are various wavelet families. An example is the Daubechies family. The families differ based on smoothness and localization of the functions in space. Wavelets are also subdivided within the families based on their levels of iteration and coefficients. Within the Daubechies family. For example, there's Daubechies 5, Daubechies 6, etc. based on their number of vanishing moments.

Wavelet Transforms provide time-frequency information and representation of signals. The most important advantage of wavelets is their high resolution in time frequency domain (Wei,2010).



(1) WAVELET TRANSFORM

The addition of all the sums of a signal $f(t)$ multiplied by scaled and/or shifted versions of the wavelet function ψ overall time is the wavelet transform of that signal.

The wavelet transform uses shorter time intervals to analyze high frequencies and longer time intervals for low frequencies. Because of this, high frequencies of short time can be successfully observed using wavelet transformation. An advantage of wavelet transformation is its ability to decompose signal at different resolutions allowing accurate feature extractions from non-stationary signals. Wavelets are grouped in families. Some of these families are Mexican Hat, Daubechies, Symlets, Meyer, Morlet, Biorthogonal, Harr, Symlets, Coiflets, and several other complex and real wavelets. Anti-symmetric wavelets work better for edge detection, and symmetrical wavelets work better for peak pulse detection (Yao,2007).

Signal processing techniques based on Discrete wavelet transform are used for reducing clutters. Over a particular level of wavelet, the processed outputs display an improvement in the peak signal-noise ratio of the data. A wavelet analysis with high order statistics is used for transient detection in low signal-noise situations (Smitha, 2017).

Below, the windowing technique is used to pre-process raw-GPR data. The figure shows wave decomposition, wavelet thresholding with denoising and reconstruction, which are the steps used in DWT processing of GPR raw data.

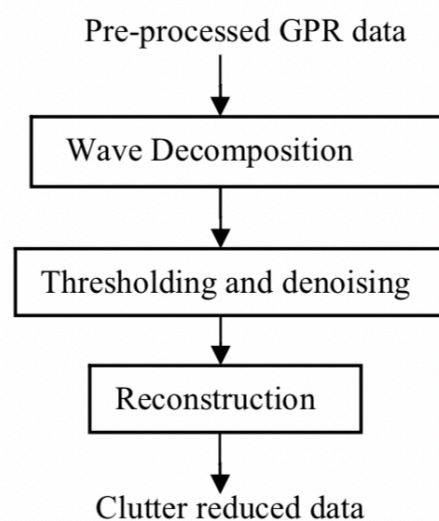


Fig. 1 Proposed steps for clutter reduction

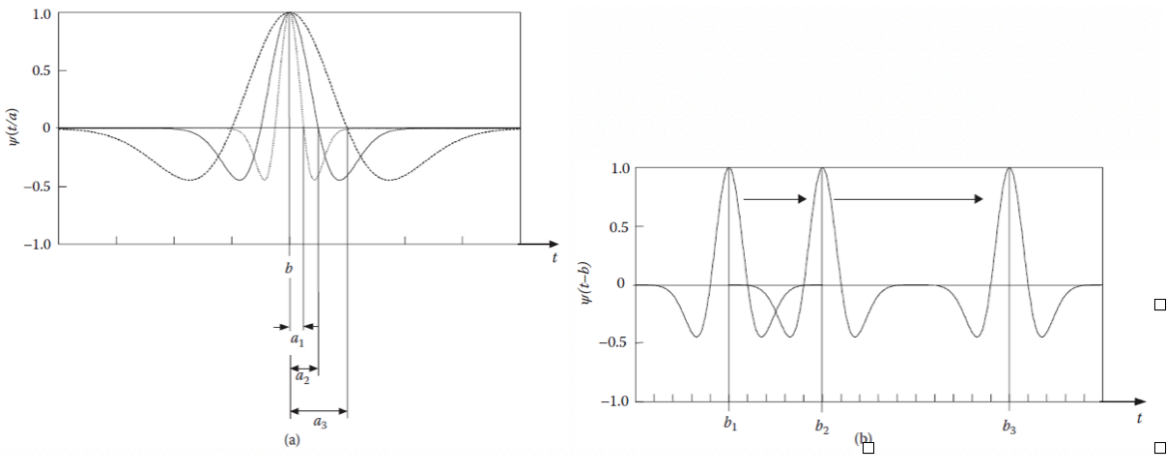
i) **Wave decomposition:** The appropriate wavelet and wavelet level is chosen in this step. Decomposition of the signal using wavelet at the selected level is done. In the decomposition process, a signal x is passed through a series of filters. The signal is broken into approximate and detailed coefficients.

ii) **Wavelet Thresholding and Denoising:** For signal denoising with the capabilities of wavelet transform thresholding is adapted. The detailed coefficients that are below threshold are nullified to remove noise. Two types of thresholding could be applied, and these include hard and soft thresholding. The coefficient values below the threshold are set to zero and subtract threshold from other coefficients is used here. This is called soft thresholding.

iii) **Reconstruction:** Wavelet reconstruction is an inverse process of decomposition. Peak signal- noise ratio is defined via mean square error. MSE is the measure of image quality in image processing (Smitha,2017).

Continuous Wavelet Transform transforms a function by integrating a wavelet family of functions. Wavelet family of functions is the modification of versions of the kernel function. The kernel function is called the mother wavelet, and it is modified by translation and compression (Wei,2010).

After picking a mother wavelet, we have to play with it to make it more compatible with our applications. We can expand or contract it, and this is also known as dilation. We can also change its position on the time axis; this is called translation. The dilation ($a_1 = a_2/2$; $a_3 = a_4 \times 2$) is shown in figure (a) and translation (from b_1 to b_2 to b_3) of a wavelet is shown in the figure (b) below



The continuous wavelet transform equation is:

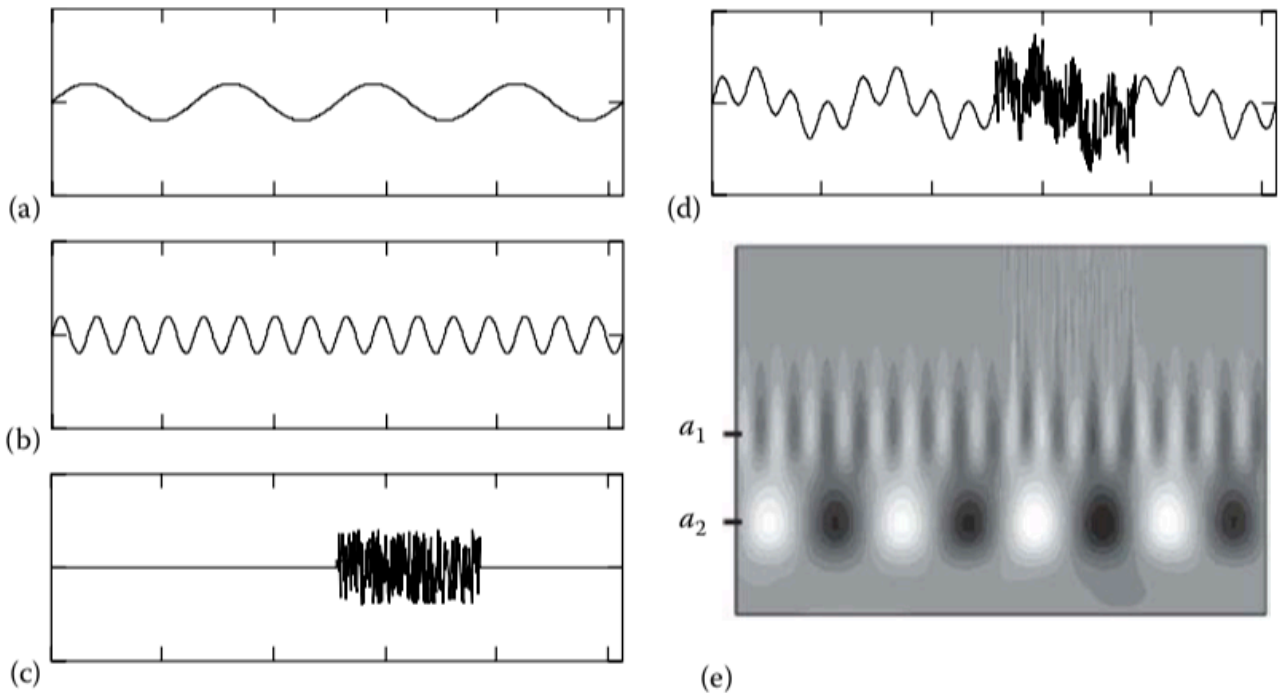
$$T(a,b) = \frac{1}{\sqrt{a}} \int_{-\infty}^{\infty} x(t) \psi^* \left(\frac{t-b}{a} \right) dt$$

Where $x(t)$ is our signal function. The equation combines the dilated and the translated wavelet.

The normalized wavelet equation is given as:

$$\psi_{a,b}(t) = \frac{1}{\sqrt{a}} \psi \left(\frac{t-b}{a} \right)$$

The figure attached below contains a composite signal and its wavelet transform plot. (a) contains a sinusoidal wave, (b) contains the same sinusoidal wave with a smaller period, (c) is a noisy signal, (d) is the combination of (a) (b) and (c), (e) is the wavelet transform plot of the combination in (d).



(2) WAVELET ESSENTIALS

A function must have these mathematical properties to be classified as a wavelet:

- Wavelets should have finite energy.

$$E = \int_{-\infty}^{\infty} |\psi(t)|^2 dt < \infty$$

- If $\hat{\psi}(f)$ is the Fourier transform of $\psi(t)$, the wavelet must have 0 frequency component. Then the admissibility constant C_g must be satisfied.

$$C_g = \int_0^{\infty} \frac{|\hat{\psi}(f)|^2}{f} df < \infty$$

- For complex wavelets, the Fourier transform should be real and shouldn't exist for frequencies less than zero

(3) COMPLEX WAVELETS

As mentioned earlier, the Fourier transform of complex wavelets does not exist for values less than zero. Amplitude and phase components of signals can be pointed out using complex wavelets. Emphasis will be laid on the complex Morlet wavelet because it will be utilized in this thesis. The complex Morlet wavelet is derived from multiplying a Gaussian function with a sine wave. The Morlet wavelet is generally given as:

$$\psi(t) = \pi^{-1/4} \left(e^{i2\pi f_0 t} - e^{-(2\pi f_0)^2/2} \right) e^{-t^2/2}$$

A more straightforward form of the Morlet wavelet is given as

$$\psi(t) = \frac{1}{\pi^{1/4}} e^{i2\pi f_0 t} e^{-t^2/2},$$

Because the part after the subtraction sign is insignificant when the central frequency given as f_0 is greater than 0 (Addison, 2017).

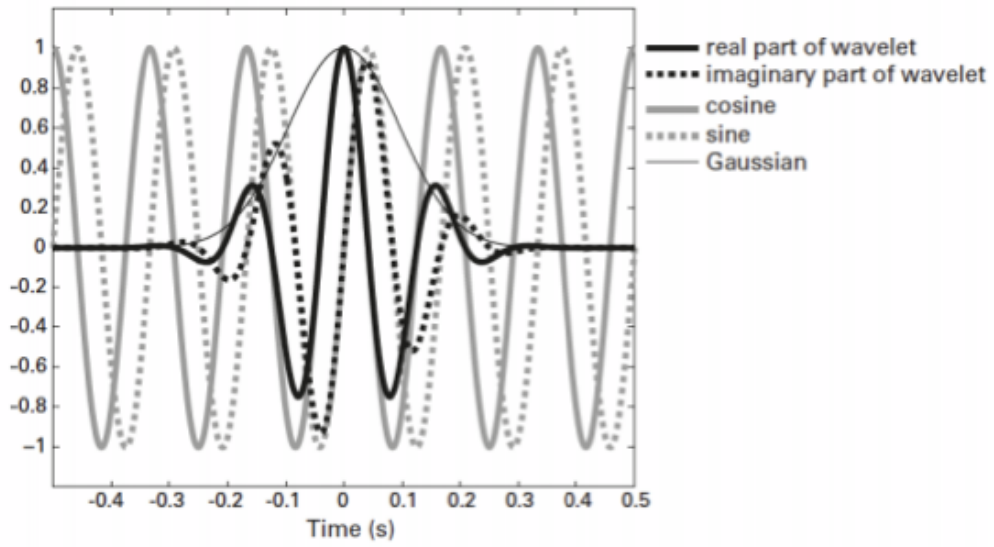
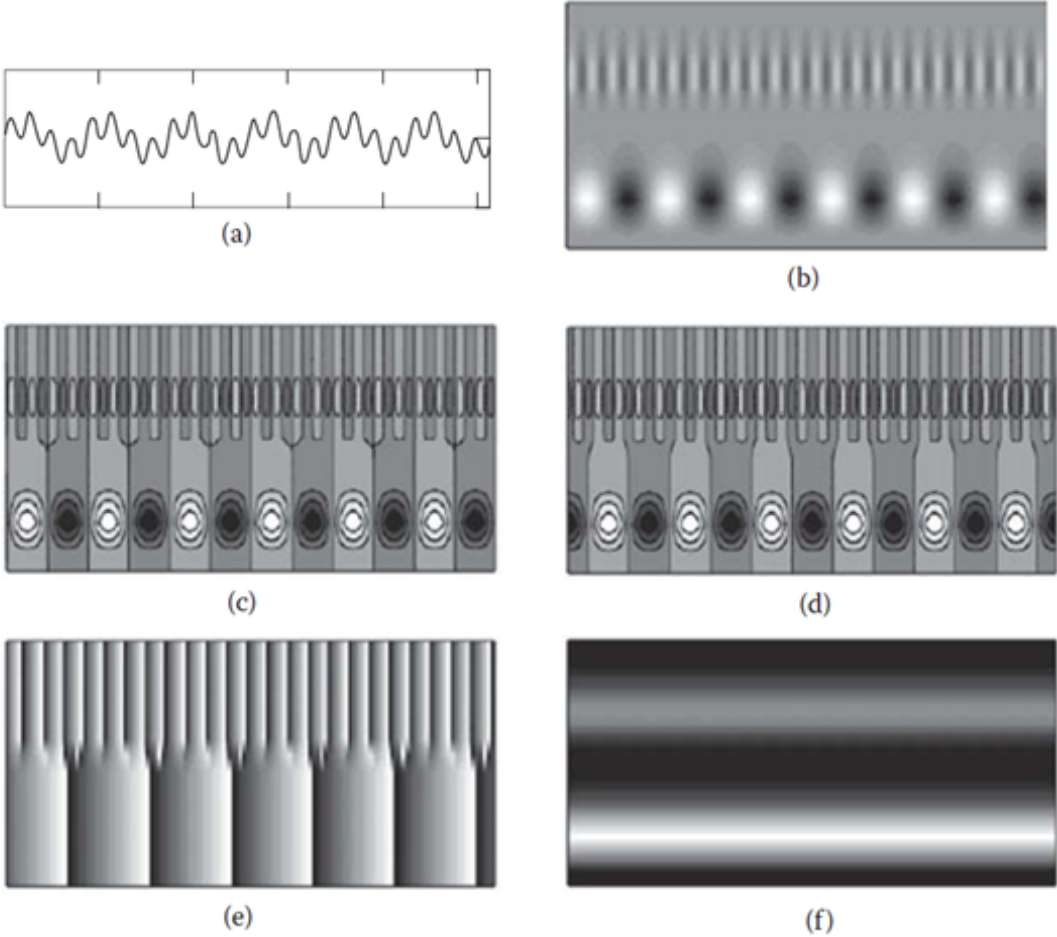


FIG 3.1. A Morlet wavelet

The wavelet analysis of a 2 component sine wave using the Morlet wave is attached in the figure below. Part (a) contains the sinusoid signal, (b) is the real part of the wavelet transform, (c) is the dark shade version of (b) with contours, (d) is the imaginary part of the wavelet transform, (e) contains the phase of the wavelets transform and (f) contains its moduli.



(Addison,2017)

(4) ENTROPY

Entropy is a measuring tool to determine the complexity of a signal. In the course of this thesis, the time domain entropy of each GPR signal will be calculated as

$$-\sum P(x)\log P(x)$$

Where P(x) is a fraction of examples in a given class

3. NEURAL NETWORKS

Artificial Neural Networks are models designed for the processing of information based on the brain and the whole biological nervous system. It is made up of the interconnection of neurons. The neural network uses algorithms inspired by the structure and function of the brain's biology to analyze data, learn from that data, and make a decisions and forecasts about new data. The algorithms or models that do this learning are based on the structure and function of the brain's nervous system. Like the brain, ANNs learns by examples. Different ANNs are designed for various applications. These applications include data classification, prediction, pattern recognition, etc. These ANNs learn by making some adjustments within the neurons while learning.

ANNs can extract useful information from complex data. This is why it is used for applications that are too complicated for humans and other methods. ANNs have various advantages. Traditional computer methods follow the instructions they are given to perform tasks while neural networks, similar to the human brain, learns and solves problems by itself.

A Neuron has inputs and one output. During training, the neurons learn to activate or not. While in use, it adapts the information it learned during training to know whether to be activated or not.

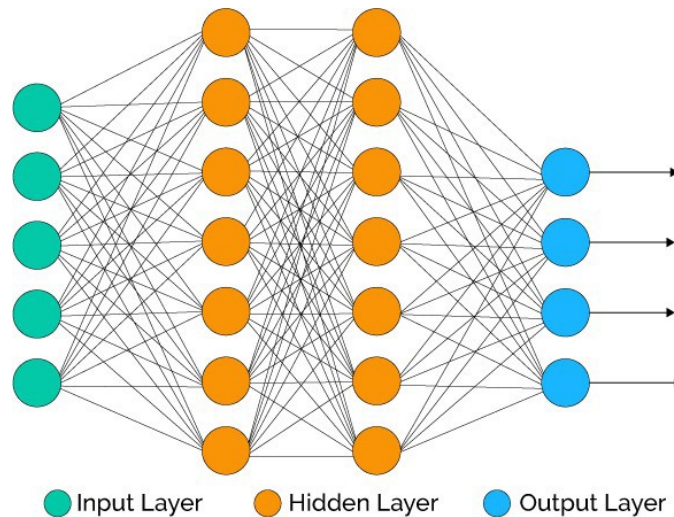
While in use, it adapts the information it acquired during training to decide whether it be activated or not.

The output of a neuron in one layer is attached to the input of the neurons in the next layer.

The architecture of a neural network determines how the neurons relates to each other. Feedforward, recurrent, and mesh architectures are the main ANN architectures.

An artificial neural network(ANN) is a computing system that comprises of a collection of connected units called neurons, which are organized into what we call layers. The input, hidden, and output layers. The input layers receive data from the outside environment. The hidden layers are where most of the networks' processing is done. There are different types of hidden layers in ANN and each type of layer is

better suited for doing some tasks than the others. Examples of these hidden layers are convolutional layers, fully-connected layers, recurrent layers, pooling layers, etc. Fully-connected layers connect each input to output within its layers, convolutional layers are best used when working with image data and recurrent layers are fully utilized when working with time-series data. The Output layer presents the final output of the network.



Let us say we have 100 different GPR Raw data of cracked and solid concrete slabs, but we do not know which is cracked and which is solid. Artificial Neural Networks can help us with the classification of these data by learning, which is cracked and which is solid based on their attributes. The neural networks get better at classification after training.

The 100 GPR Rawa data are used as the input data, which is put through the neural network to get an output, which is the correct classification an of either solid or cracked slab. For this network, the input layer will consist of 100 neurons, the hidden layers will have neurons depending on the attributes of the data, and the output layer will consist of 2 neurons for solid or cracked.

The input data is fed into the network and several matrix operations are performed on it at each layer. A Bias is added to the dot product of the input and weights; then it is passed through an activation function. The output of this is served as an input to the next layer, and a similar process takes place. The output of a node is the multiplication of the activation function and the weighted sum of all the inputs to that node. The output value is passed as input to the nodes in the next layer. As the model learns during training, the weights are updated and optimized so that the input data is

mapped to the correct prediction class. This updating of the weights is essentially what we mean when we say that the model is learning. At the end of each epoch during the training process, the loss will be calculated using the network's output predictions and the true labels for the respective input.

This iteration happens depending on the number of layers we have. The output is the classification, solid, or cracked. We find the difference between the desired output and the output we got and use the error during backpropagation. We put the error back into the network in the opposite direction for the network to learn from it. After some iterations, the network does a better job at classification by adjusting its parameters to fit our data (Silva,2017).

New developments in computers and ANNs have changed health analysis of bridges using GPR. ANNs are very useful because they can be trained to ignore the noises that can affect GPR Data. They can extract valuable features from complex data. Compared to other methods, they have high pattern recognition performances, which make them very useful in classification. Other advantages of the neural network include real-time processing and adaptability (Kilic,2014).

These are some NN related terms that need to be known;

Weight: The value of the strength of the connection between two nodes. Initial values at first epoch are random. Values are optimized during training.

Updated weight = old weight - (learning rate * gradient)

Activation function: Inspired by biological activities in our brain where different stimuli activate different neurons. It is a function that maps a node's input to its corresponding output. An example is the sigmoid function which transforms negative inputs into a number close to 0, positive inputs into a number close to 1 and numbers close to zero into a value between 0 and 1.

Epoch: A cycle. Once all of the data points in a dataset have been passed through the network, we say that an epoch is complete. Following the end of each epoch the model gives an output for the given input.

Learning rate: a small number ranging between 0.01 - 0.001

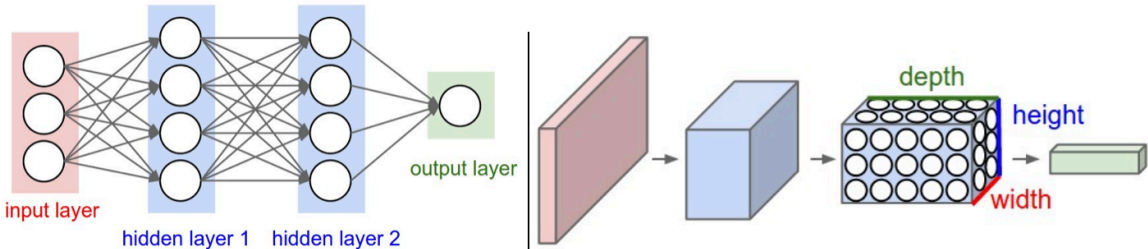
Filter: a matrix (e.g., of size 5*5) that include weights which change with every iteration over the training data to identify the essential features in an image. These weights are multiplied by the adjacent image pixel values, and all of these

multiplications are summed up to represent a single number. This is done for every location in the input image, producing an activation map or a feature map.

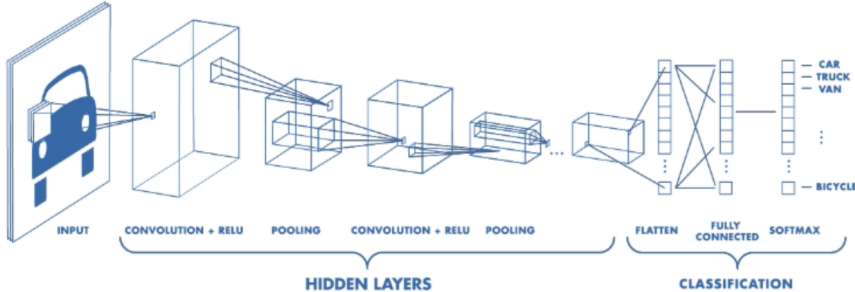
4.CONVOLUTIONAL NEURAL NETWORKS

A CNN is an ANN that specializes in picking out or detecting patterns. This makes it very useful for image analysis. CNN is different from normal ANNs because it has convolutional layers. The name is derived from CNN’s vital operation of convolution. Unlike the normal ANN where inputs are operated on by passing them through a sequence of hidden layers, where every layer consists of neurons linked to each other, The CNN has a different architecture.

CNN layers are arranged in 3 dimensions (Length, breadth, depth). The neurons in one layer are only connected to a small part of the next layer, unlike in the ANN where they are connected to all of it. The final output layer makes the image into a smaller single vector.

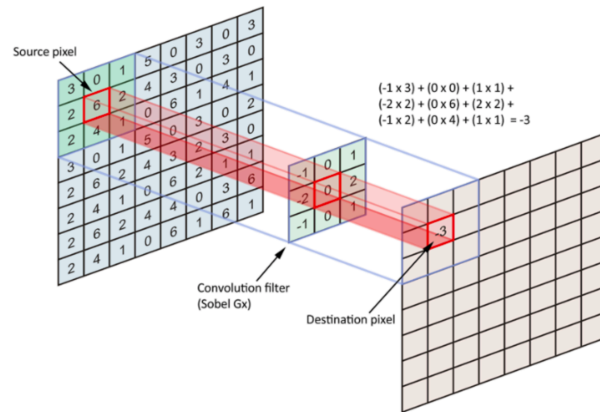


CNNs generally have two parts.



1. **The Feature extraction Part:** This is the part where all the features are identified. If we had the image of a car, for example, the color, the number of tires, the shape of the car, etc. are identified in this part. The convolutions and pooling are done in this part.

Convolution is a mathematical operation of merging two functions to create a 3rd function. In CNN, it joins the input data using a filter/kernel to create a feature map. The filter is shadowed on the input, and matrix multiplication is computed. The result is put into the feature map.



The convolution operation is repeated many times using different filters to obtain different feature maps. All the feature maps are combined and used as the output of the convolution layer.

CNN's also have activation functions. Its purpose is to make the output non-linear to speed up the learning and improve performance. The Rectified Linear Unit (ReLU) is the most commonly used activation function.

The feature map is smaller in size than the input. To prevent it from shrinking, we add numbers to the feature map. This is known as Padding. An example of this is Zero-Padding, where we add 0s to the feature map.

Pooling is cutting of the dimensions (length, breadth, width) by reducing unimportant data and saving only the extracted features. It controls overfitting and saves training time. Examples of this are Lp pooling, stochastic pooling, spectral pooling, mixed pooling, max pooling, average pooling, etc. The pooling layer usually comes after the convolutional layer.

2. **The Classification part:** The extracted features are classed by the fully connected layers. The fully connected layers only accept one-dimensional data. Therefore, the 3D data from the previous layers are flattened. These layers are called fully connected because just like in a standard ANN, the neurons of these layers are fully connected.

CHAPTER 4

EXPERIMENTS AND RESULTS

1. EXPERIMENTAL SETUP

Materials were set up in the lab to carry out experiments. A solid concrete cuboid slab, a concrete cuboid slab with 1mm crack, a concrete cuboid slab with 1cm crack, a concrete cuboid slab with 1cm crack, a solid concrete cylindrical slab, a cracked concrete cylindrical slab, wooden, and concrete cubic slabs.



FIG 4.1. Experimental Setup

After conducting extensive research under the literature review section, 3 NDTs listed below with reasons were used for the experiment

Visual Inspection: Visual inspection is a quick and cheap way of detecting cracks, but it is not reliable because it recognizes only external cracks, and it is also viable to human error.

Thermal Camera: This is a quick, portable and inexpensive method of surface and internal defect detection. It generates high penetration depth, but it is affected by temperature and weather conditions.

Ground Penetrating Radar: GPR is straightforward to use and non-time consuming NDT. It is also accurate because of its high data acquisition rate and sensitivity to variations of permittivity. Nonetheless, the interpretation of GPR data can be difficult, and GPR devices are expensive.

(1) VISUAL INSPECTION

- Preparation of equipment and documents (Concrete slabs and wood)
- Safety Precautions (Wearing protective equipment)
- Inspection of Materials used (Cracked & solid concrete slabs and woods)
- Records (Writing down observation and photographs)
- The cracks, material type, and some other features on the surface of the slabs were identifiable visibly.



FIG 4.2. Cracking a slab

(2) THERMAL CAMERA

A Testo 875-1i - Infrared camera with SuperResolution owned by Dr. Gökhan Kiliç was used. It has a built-in digital camera which allows us to see both the thermal image and real image to make documentation, more accessible. It has up to 19,200 temperature measuring points which give more detailed images; its thermal sensitivity is <50 mK which allows us to see even the smallest temperature difference, It has solar mode and automatic hot/cold spot detection. It has a measuring range of -30 to $+350$ °C. Moreover, it is used in detecting structural defects and ensuring construction quality.



FIG 4.3. Thermal Camera

- First the cracked and solid concrete slabs were prepared as well as the wood for thermal camera imaging.
- Safety Precautions were taken by wearing personal protective equipment.
- The materials were inspected using the thermal camera. Thermal images of the cracked, solid, and wooden materials were taken.
- The order in which the thermal images were captured was written to prevent mixing up the records



FIG 4.4. Thermal camera images

(3) GROUND PENETRATING RADAR

A TR-HF 2 GHz GPR device owned by Dr. Gökhan Kiliç was used. It has a 2 GHz antenna, Panasonic CF-19 Data logger, 1 Radar control Unit with one operating channel, 13x12x8 antenna size, and 1.3kg antenna weight. This GPR kit allows the acquisition of data with the highest resolutions. It reveals deep and shadowed targets in half the acquisition time compared to standard devices due to its full-polar antenna. It has many surveying abilities including; inspection of concretes for the location of voids, concrete thickness, integrity, inspection and analysis of old structures and monuments, inspection of floors and walls for location of pipes, and



FIG 4.5. GPR Device

wires.

- First the cracked and solid concrete slabs, as well as the wood for the GPR inspection, were prepared.

- Safety Precautions were taken by wearing personal protective equipment
- The materials were inspected transversally and longitudinally across the slabs using the GPR. We took GPR reading of the cracked, solid, and wooden materials.
- The order in which the thermal images were captured was written to prevent mixing up the records



FIG 4.6. Taking GPR Reading

The GPR Raw-Data was extracted from the device using GRED HD 3D - Advanced GPR processing and imaging software. The various B-Scan images, Average trace spectrums (A-Scans) images, and signal data were extracted.

2.RESULTS AND ANALYSIS

In previous chapters, advanced NDTs were discussed with their various advantages and disadvantages. Wavelets, artificial neural networks, and other signal processing methods were discussed, and the experimental setup was described. Following this chapter, the results of the experiments will be presented.

(1) VISUAL ANALYSIS OF RAW-DATA

After the data was extracted from the GPR device, it was separated into groups to be fed into the Neural network. The data was classified as cracked, no crack, cube, cylinder, wood, etc. to use as target.

As mentioned in the literature review, GPR Data is difficult to understand or classify without a skilled operator. So with the help of Dr. Gökhan Kiliç, the data were visually analyzed and classified . While looking at the waves in the B-scan, one can see that the concrete is cracked, and point out the location of the crack.

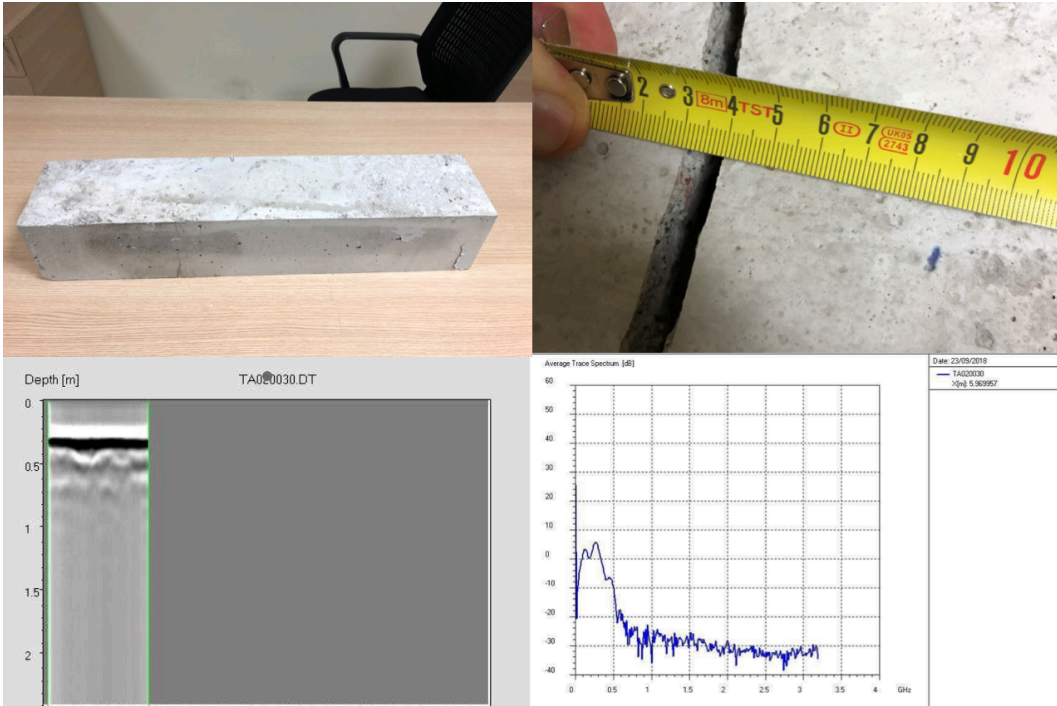


FIG 4.7. Concrete slab with 1cm crack, B-scan and average trace spectrum

The slab attached in the figure is 55cm long, 15 cm wide and has a height of 15 cm. It is made of concrete, and it was cracked using a hammer for the experiment. It was first inspected visually, and the crack was not clearly visible because it was very

small. The slab was scanned using a TR-HF 2 GHz GPR . The scans were saved as raw data for processing to get relevant information. The B-scan and trace spectrum were also extracted, which are also included in the figure.

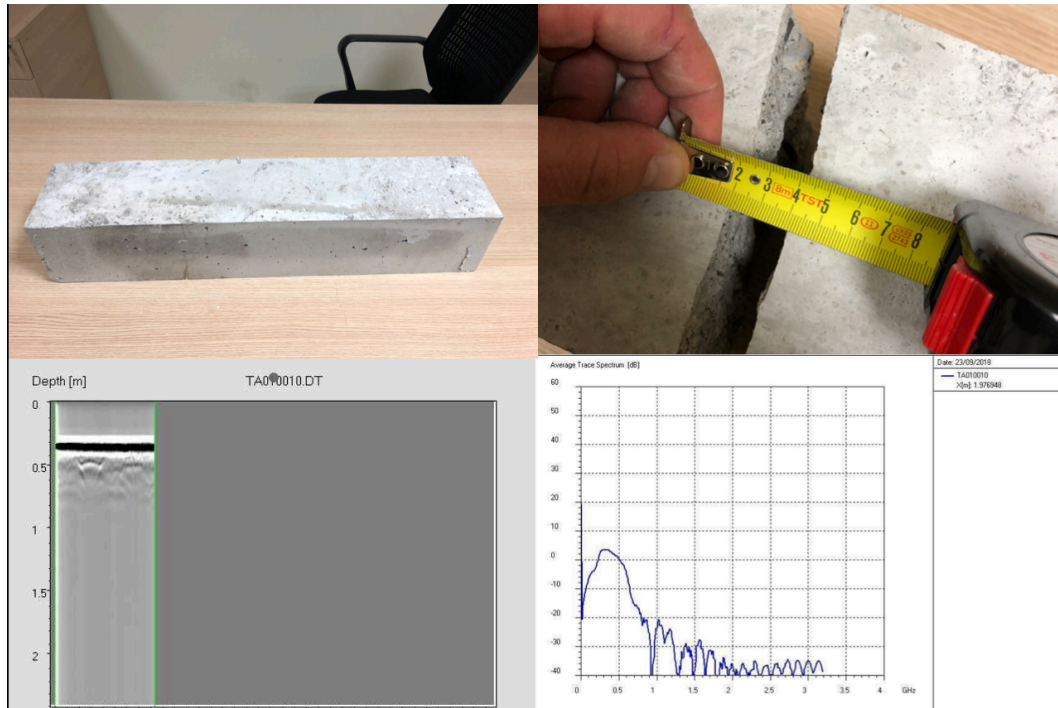


FIG 4.8. Concrete slab with 2cm crack, B-scan and average trace spectrum

The slab attached in the figure is also 55cm long, 15 cm wide and has a height of 15 cm. It is also made of concrete but it has a bigger crack than the slab in figure 4.1. By Inspecting the B-scan, one can also tell that this slab is cracked and the crack is larger than the crack in this figure and the previous one because the hyperboles in the waves are more deteriorated.

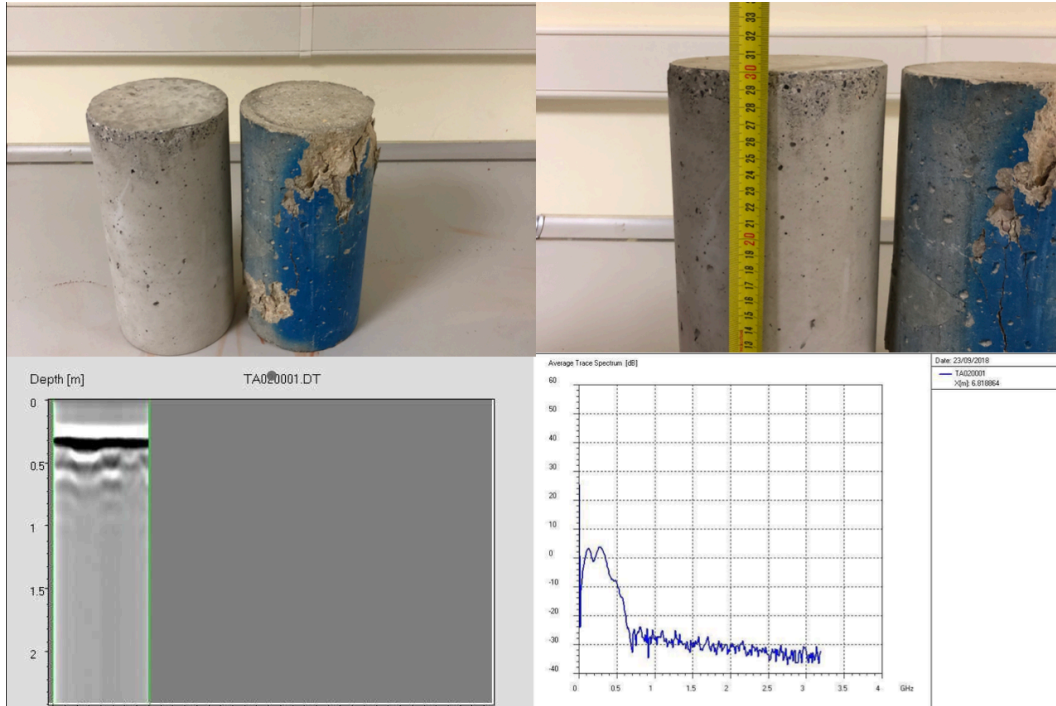


FIG 4.9. Cylindrical concrete slab with no crack, B-scan and average trace spectrum.

The slab in the figure is a 30cm long cylindrical concrete slab. By Inspecting the B-scan, one can tell that this slab has no crack and cylindrical.

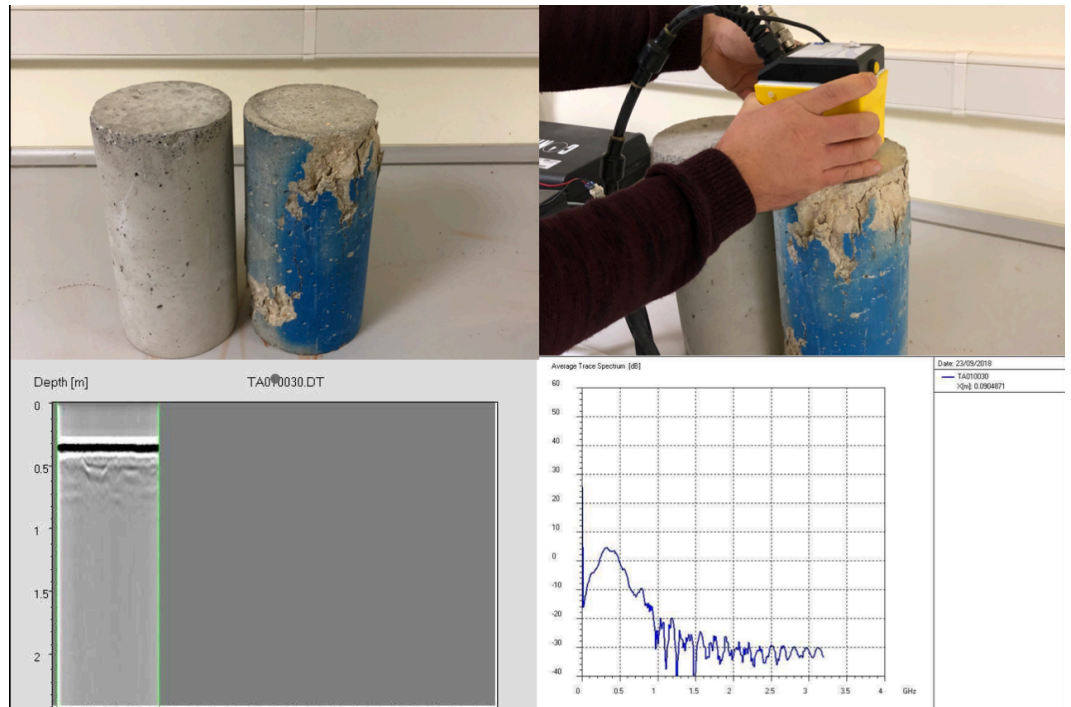


FIG4.10. Cracked cylindrical concrete slab, B-scan and average trace spectrum.

The slab in the figure is a 30cm long cylindrical concrete slab. By inspecting the b-scan, one can also tell that this slab is cracked and cylindrical. The B-scan is similar to the one in the previous figure in shape because they are both cylindrical, but the hyperboles in the waves are different because this one is cracked.

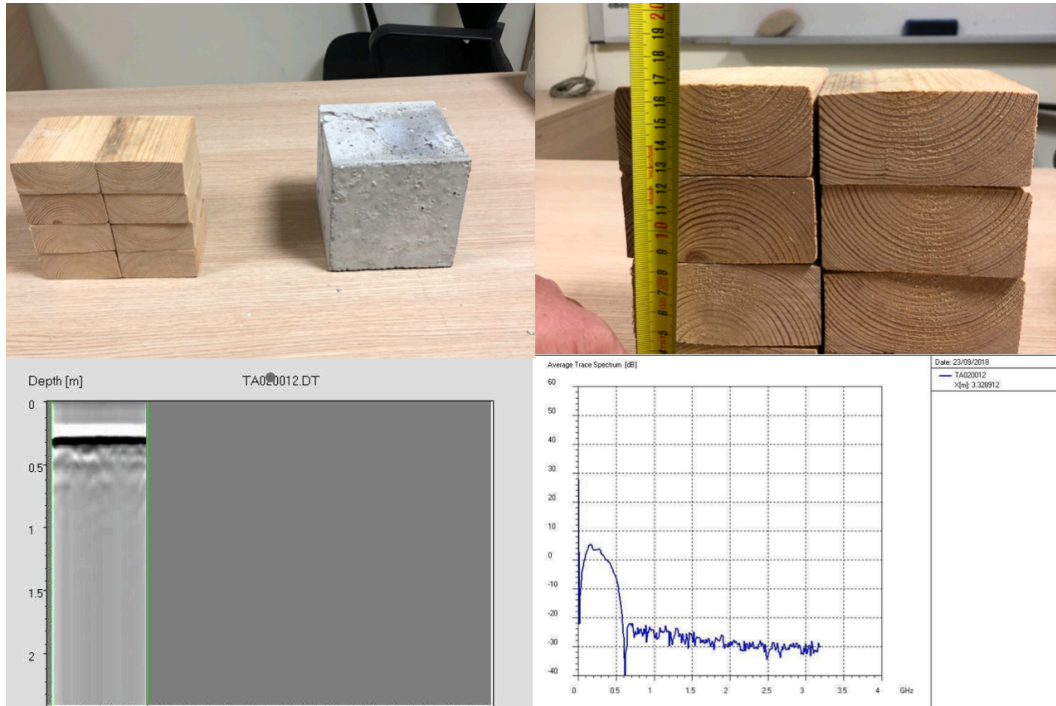


FIG 4.11. Wooden slab, average trace spectrum and B-scan

The slab in the figure is approximately a 15cm by 15cm by 15cm wooden slab. By inspecting the b-scan, one can also tell that this slab is wooden. The B-scan almost has no hyperbolic waves compared to the other figures because of the wooden material.

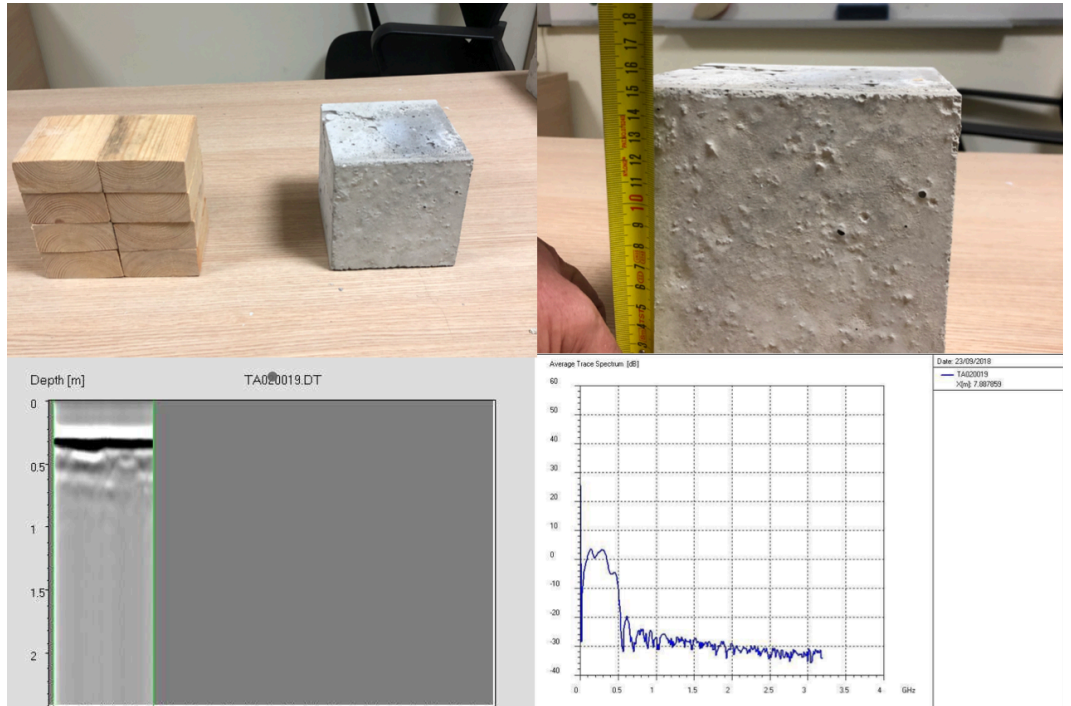


FIG 4.12. Solid cubic concrete slab, B-scan and average trace spectrum

The slab in the figure is approximately a 15cm by 15cm by 15cm solid concrete slab. By inspecting the B-scan, one can also tell that this slab is concrete and solid. The shape of the b-scan is similar to the one in the previous figure because they are both cubics, but it is different because they're made of different materials.

(2) VISUAL ANALYSIS OF SIGNALS

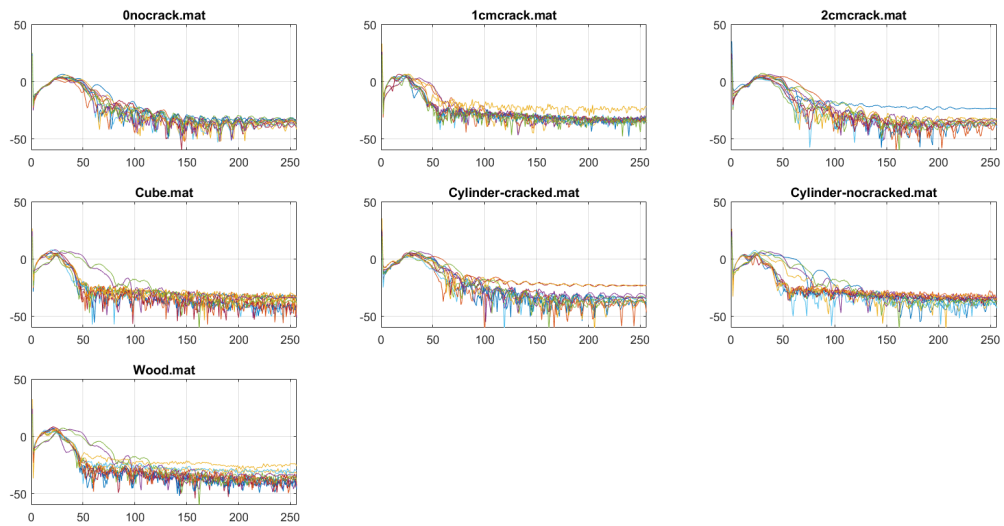


FIG 4.13. Plot of all signals

All the GPR Signals were plotted together according to their classification in Matlab to see if it is possible to determine a difference by inspecting it visually.

From looking at the different plots, one can see that there is no significant difference between the different classes of signals.

(3) THERMAL IMAGE ANALYSIS

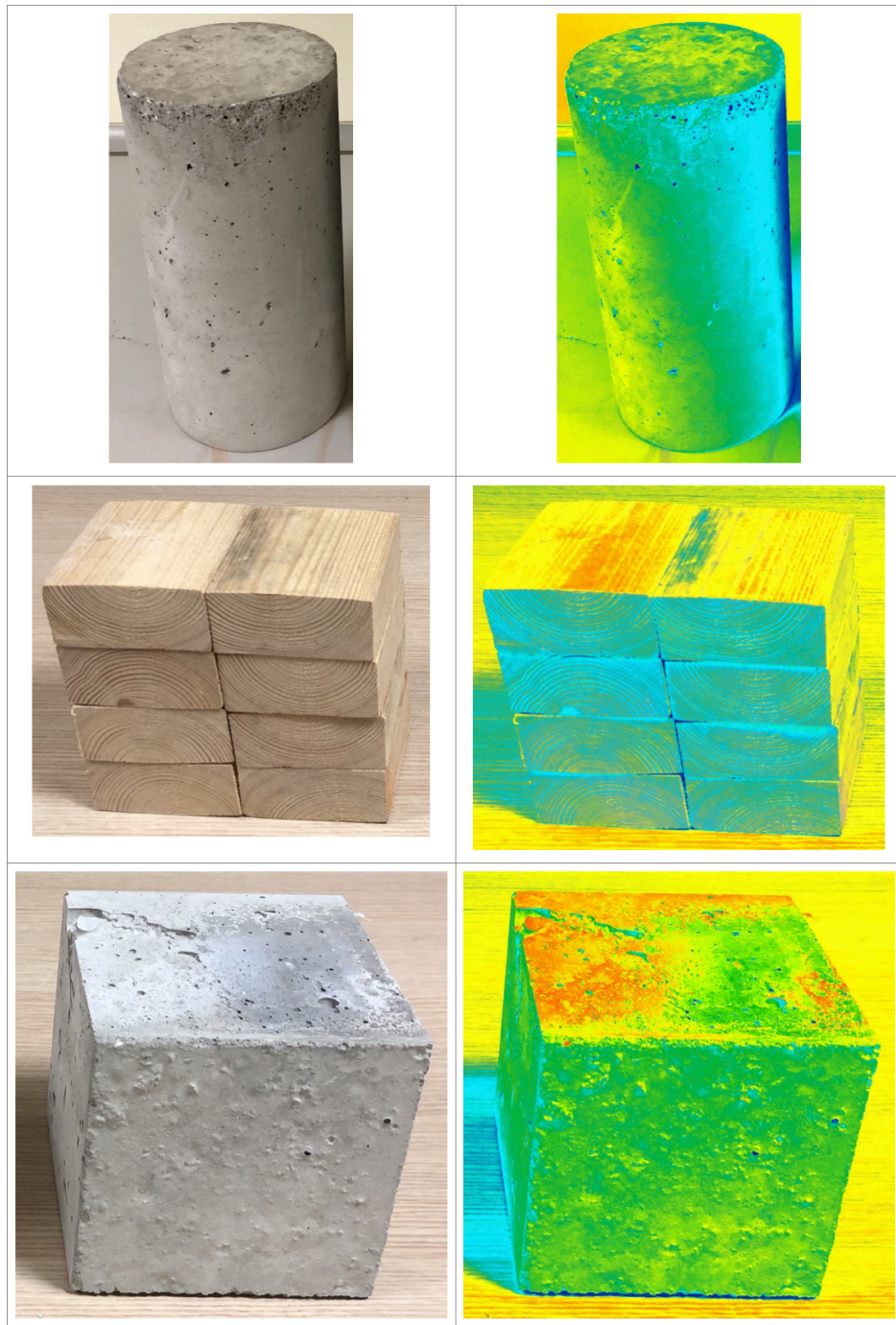


FIG 4.21. Thermal camera images

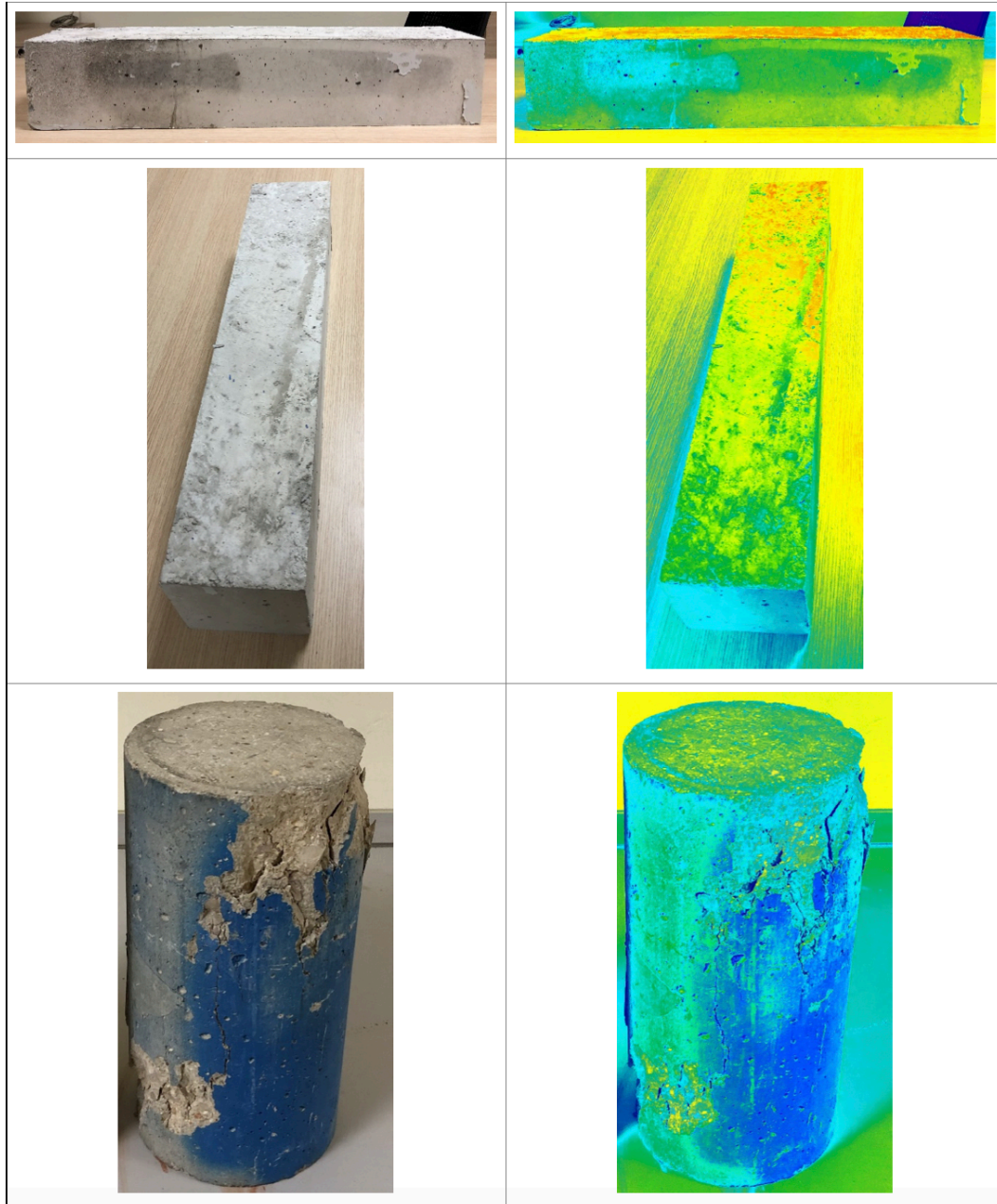


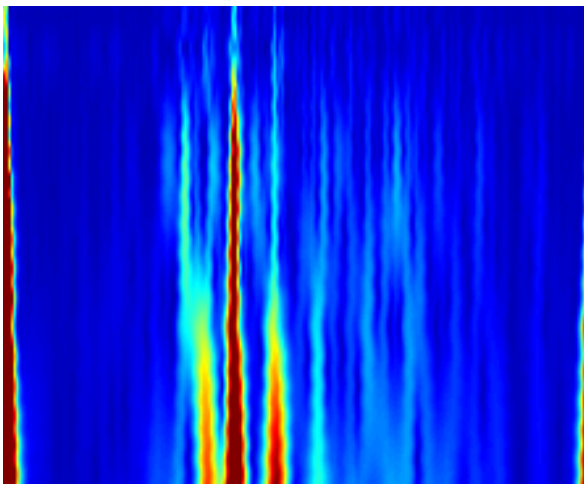
FIG 4.22. Thermal camera images

The figures above are the results from our thermal camera. Looking at the normal images, the internal cracks and difference in concrete quality cannot be spotted. From the difference in color layers and grains of the thermal camera images, the difference becomes clearer. For the purpose of future work, thermal camera images will be useful.

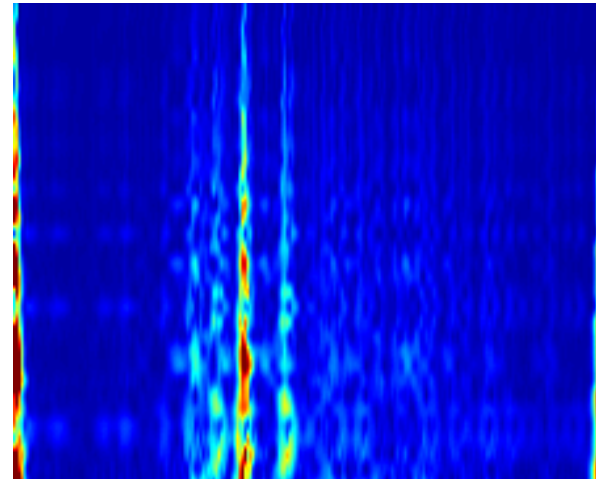
(4) WAVELET ANALYSIS OF SIGNALS

Wavelet transform was done to the data to accomplish a better analysis. The complex wavelet transform was applied to the data. The complex Morlet was used because of its different frequency modulations, and its ease of modification. The complex Gaussian was also used to have a variety.

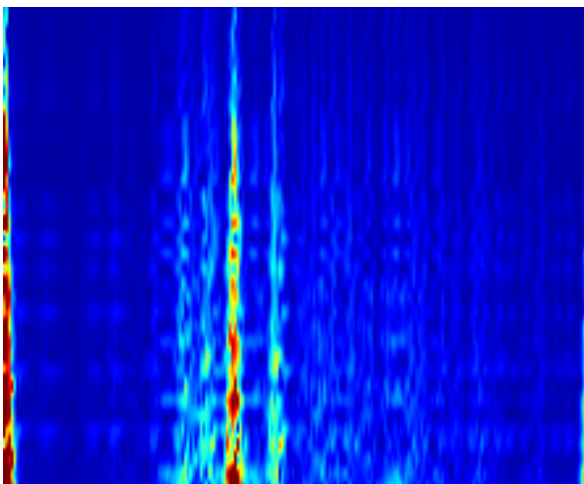
The figures attached below are wavelet transforms of signal from a cylindrical slab with no crack.



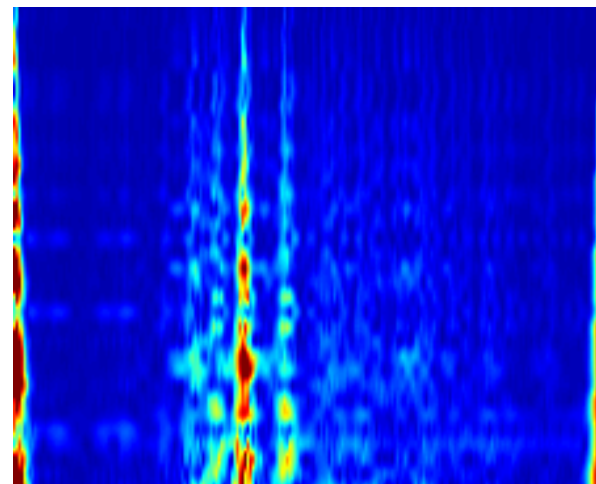
COMPLEX GAUSSIAN 8



COMPLEX MORLET 1-10

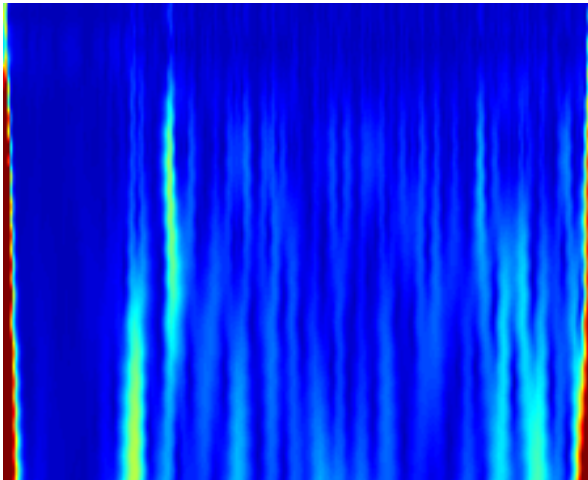


COMPLEX MORLET 1-20

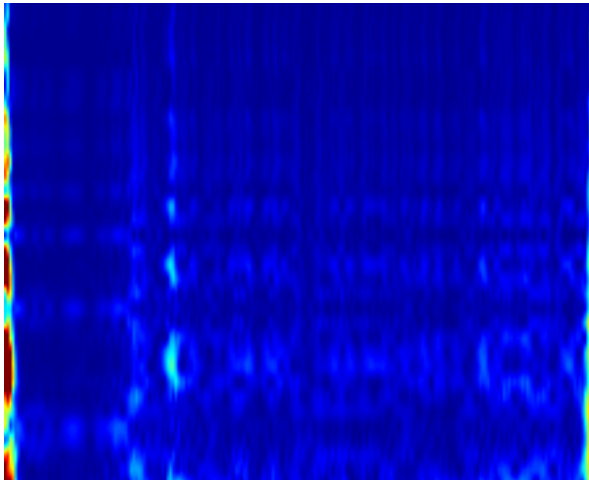


COMPLEX MORLET 2-10

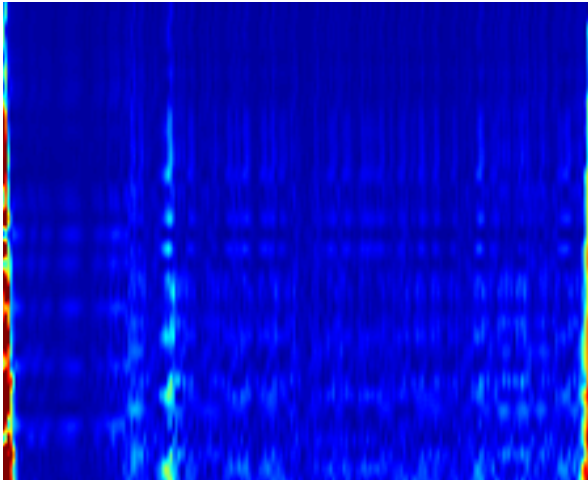
Now compare with wavelet transforms of signal from a cracked concrete slab.



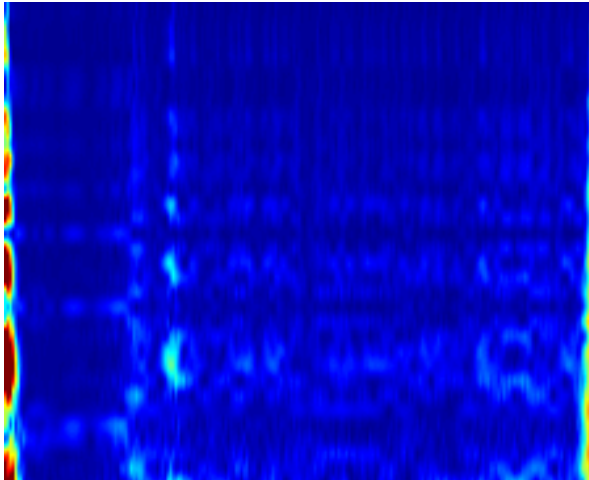
COMPLEX GAUSSIAN 8



COMPLEX MORLET 1-10



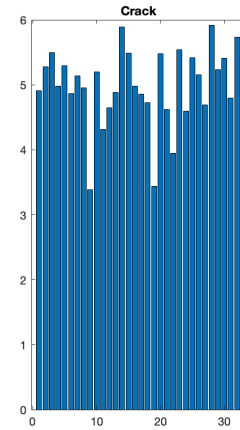
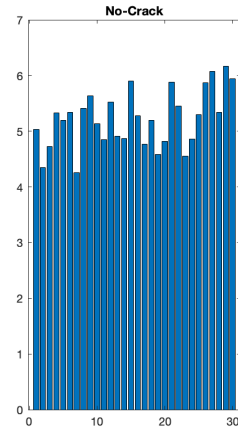
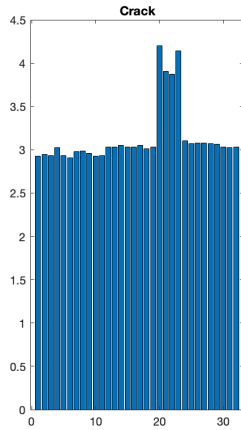
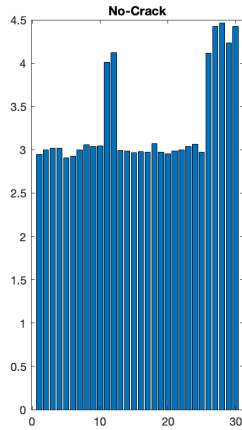
COMPLEX MORLET 1-20



COMPLEX MORLET 2-10

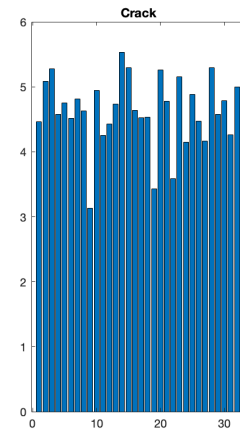
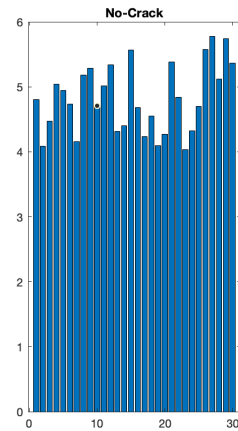
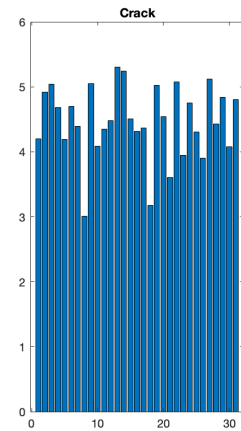
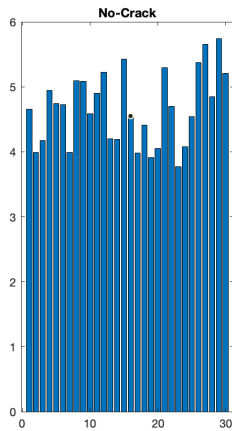
(5) ENTROPY ANALYSIS

To better analyze the data, the entropy of the raw-data images and the various wavelet transforms of the Data was calculated on Matlab.



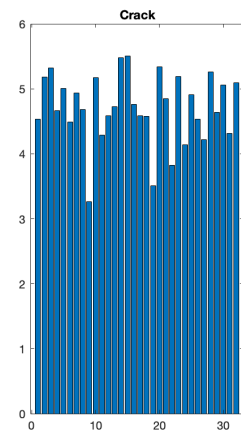
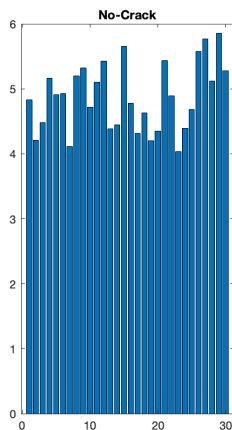
RAW-DATA

COMPLEX GAUSSIAN 8



COMPLEX MORLET 1-10

COMPLEX MORLET 1-20



COMPLEX MORLET 2- 10

Looking at the raw-data entropy plots, it can be told that the complexities of the crack and no crack data plots are very similar. Comparing it with the entropy plots of the various wavelet transform results where the difference in the complexities can be seen, it is clear that using the wavelet transform results for the classification would give better results. Therefore, the wavelet transform images were used for the next step.

3.CNN CLASSIFICATION

The dataset comprises of 169 wavelet images of cracked GPR data and 160 wavelet images of wavelet images of GPR data with no crack.

The data was loaded as an image data store, and the neural network divides the data into training and validation datasets. GoogleNet was chosen as the pretrained network and the final two layers were replaced with new layers readjusted to a dataset to classify the images. The network was trained, and classification accuracy was calculated.

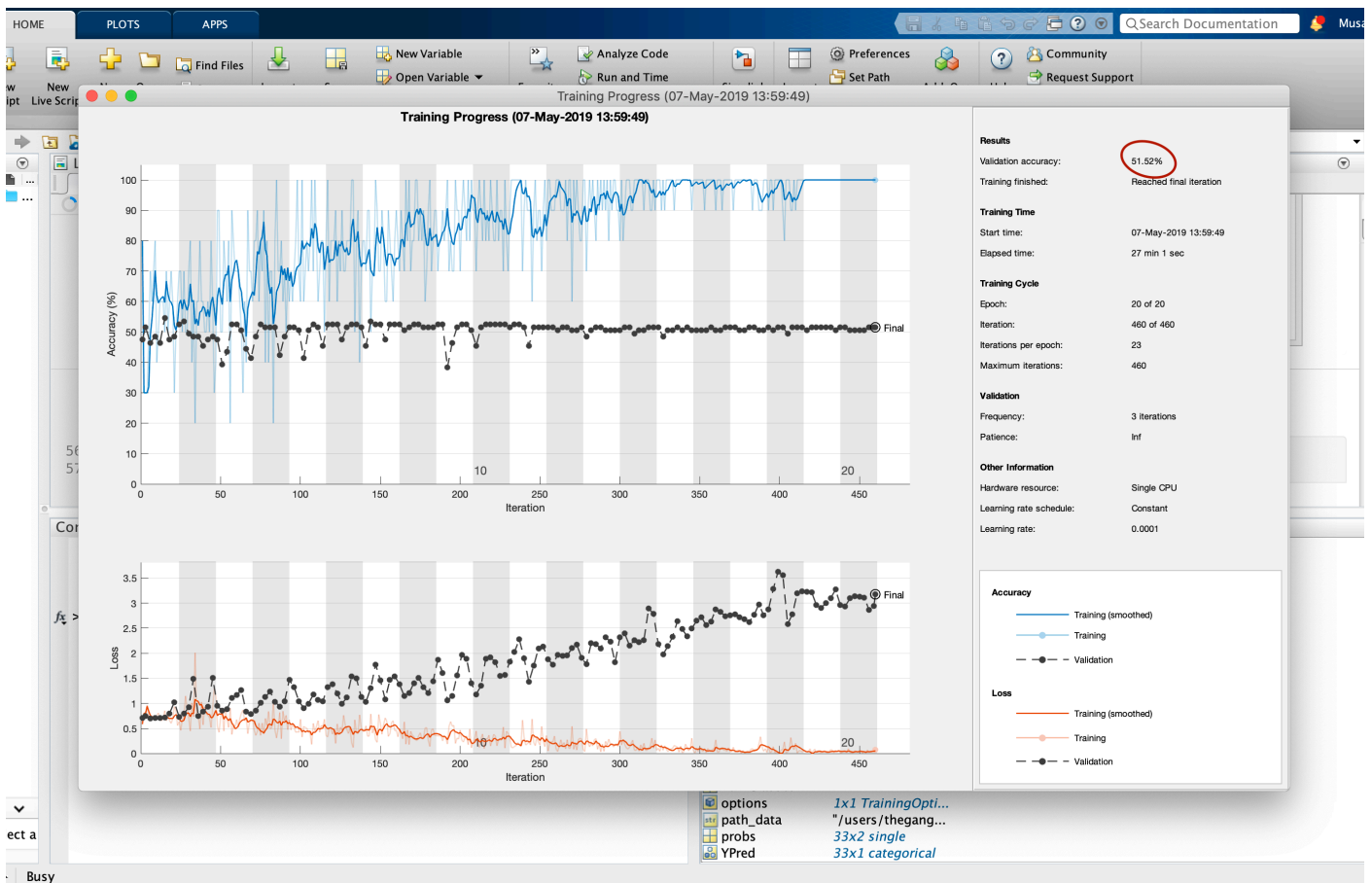


FIG 4.14. CNN classification results

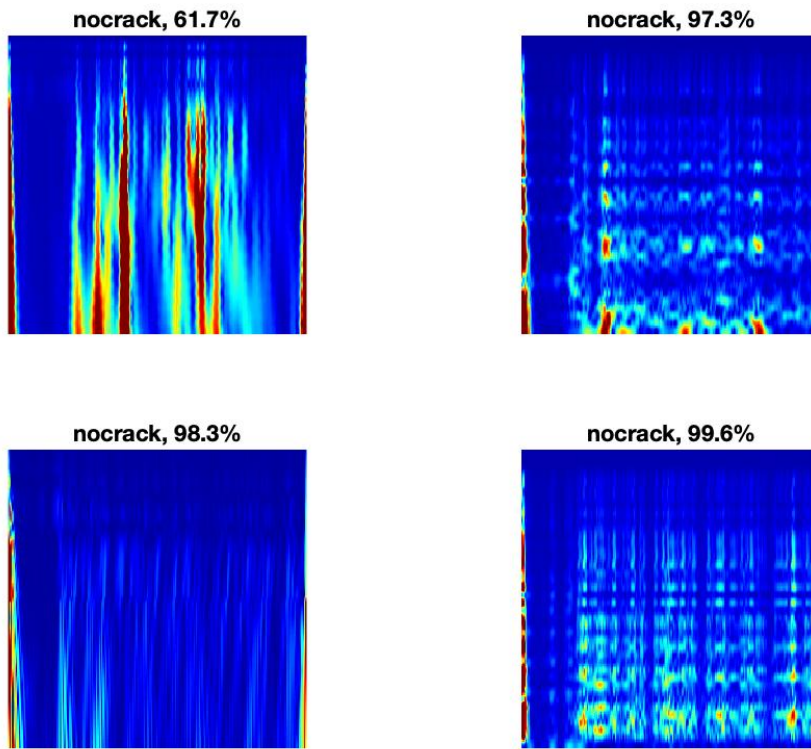


FIG 4.15. Classification accuracy

4. CASE STUDY

The lab experiment results were used to test the effectiveness of the methods. The size of the slabs and cracks were very small, resulting in poor CNN classification results. Nonetheless, there were high signs of success.

A case study bridge used for previous research works was used to test the methods on a big scale. The Pentagon Road Bridge in the south-west of the UK. The bridge is 66.7m long and 14.29m wide. The bridge was assessed using 600MHz, 1GHz, 1.5GHz, 2GHz, 4GHz antennas giving different B-Scans. The higher the antenna, the better the resolution but the lower the antennas, the better the penetration depth.



FIG 4.16. The pentagon bridge

The bridge was constructed in 1975, therefore it has many cracks, moisture ingress and other anomalies which can be detected by analyzing GPR Raw-Data.

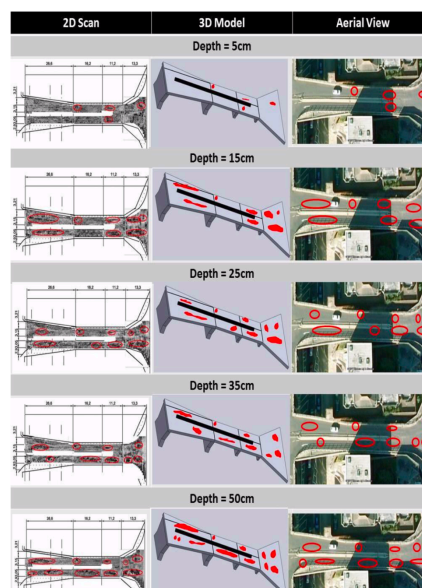
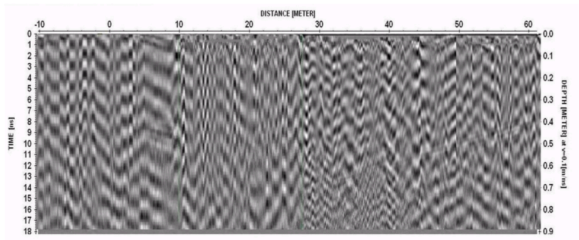
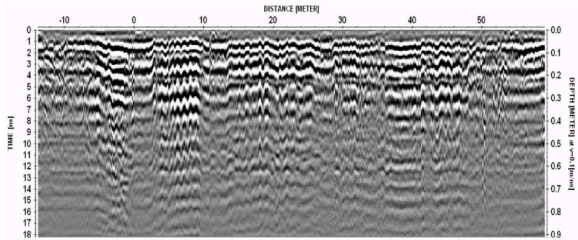


FIG4.17. Vertical slices of bridge data(left),
Computer model of position of
anomalies(middle), real life location of
anomalies(right)

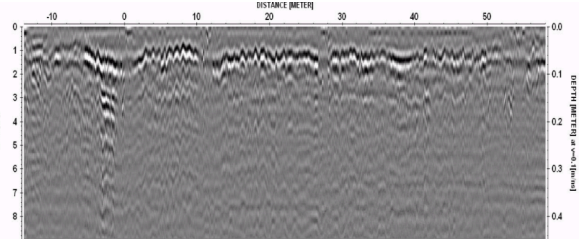
There are many anomalies at different locations and depths which can be identified from the various B-scan images. The B-Scans from 600MHz GPR antennas provide more depth (about 50cm) information with low resolution compared to other antennas. The 1GHz antennas has 35cm depth range. The 1.5GHz has 25cm, the 2GHz has 15cm and the 4GHz has a depth range of only 5cm but has the best resolution.



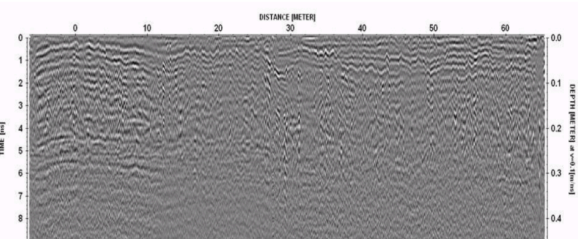
600MHZ B-SCAN



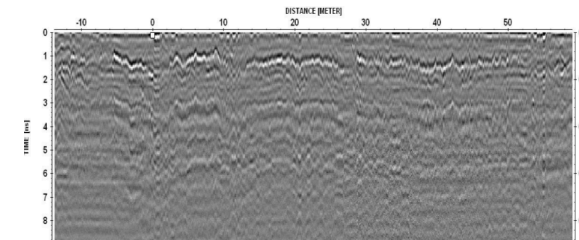
1GHZ B-SCAN



1.5GHZ B-SCAN



2GHZ B-SCAN

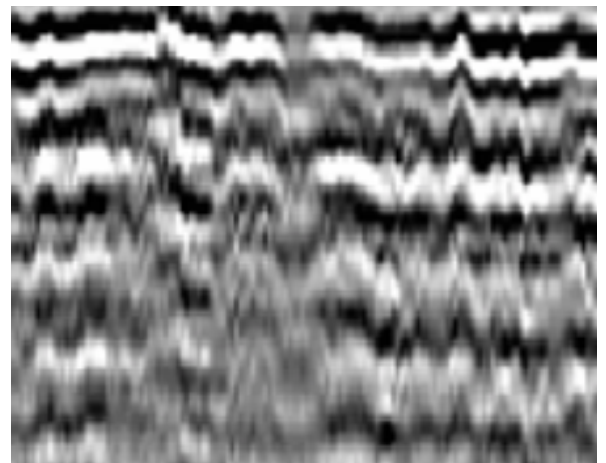


4GHZ B-SCAN

Each B-scan contains data from approximately 70m length of the bridge. Some parts of each b-scan contain anomalies while other parts are normal. The B-scans were divided into 10m each at half the timeframe to provide 14 parts for every b-scan. There are 36 different B-Scans of the bridge gotten using different antennas at different positions. Multiplying that with 14 parts for every b-scan, that gives 504 data images to work with. The data was grouped into two, normal and parts with anomaly with reference to the old research work.



NORMAL PART



PART CONTAINING ANOMALY

The data was fed as input into a pre-trained CNN to check the classification accuracy.

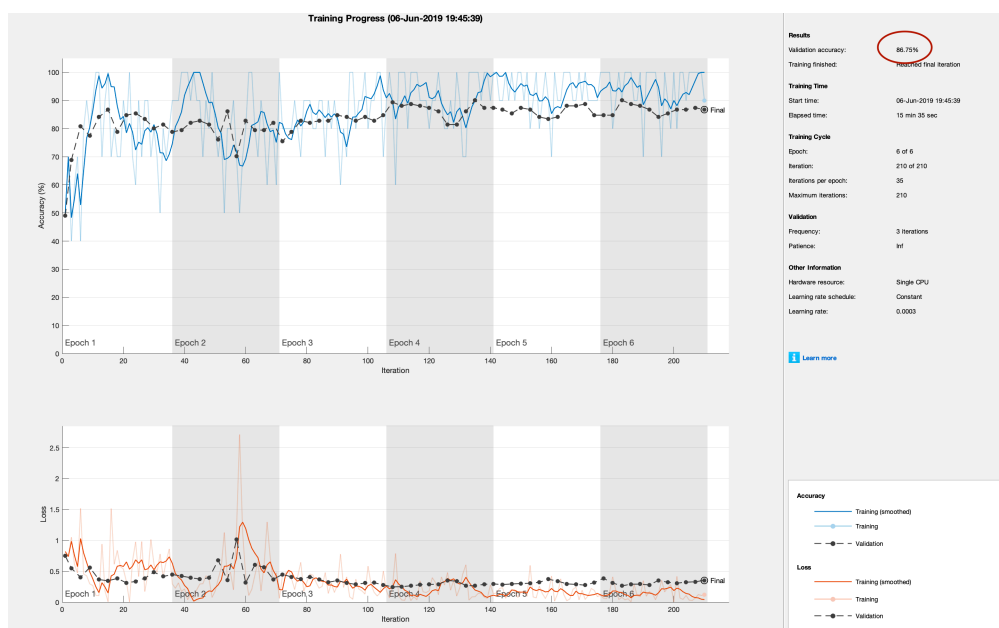
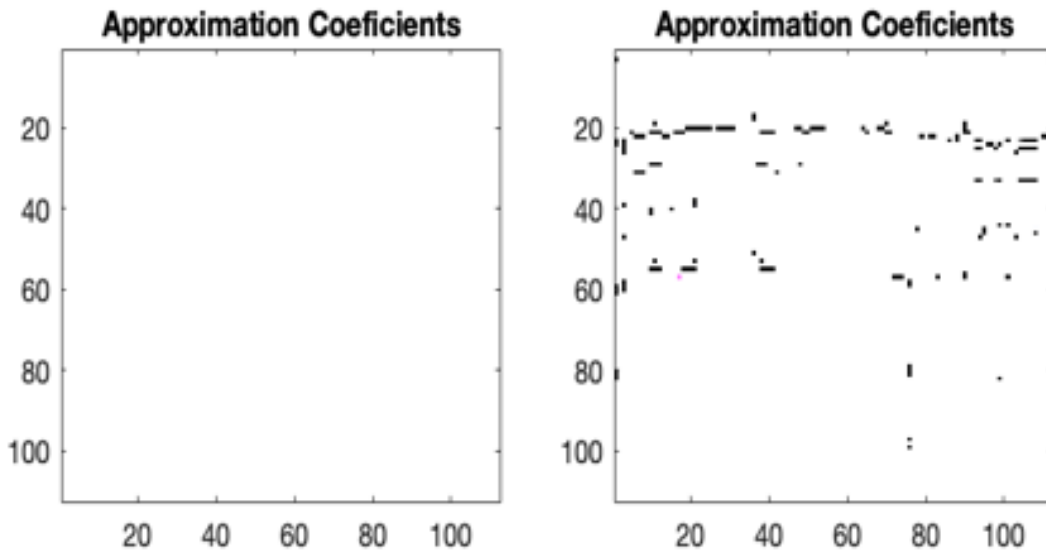


FIG4.18. CNN classification result

The classification result is significantly better than that of the lab experiment results.

This shows that the CNN works better in bigger scale.

Wavelet transform was done to the data to get a better analysis. Discrete wavelet transform was done using level 10 Daubechies wavelet.

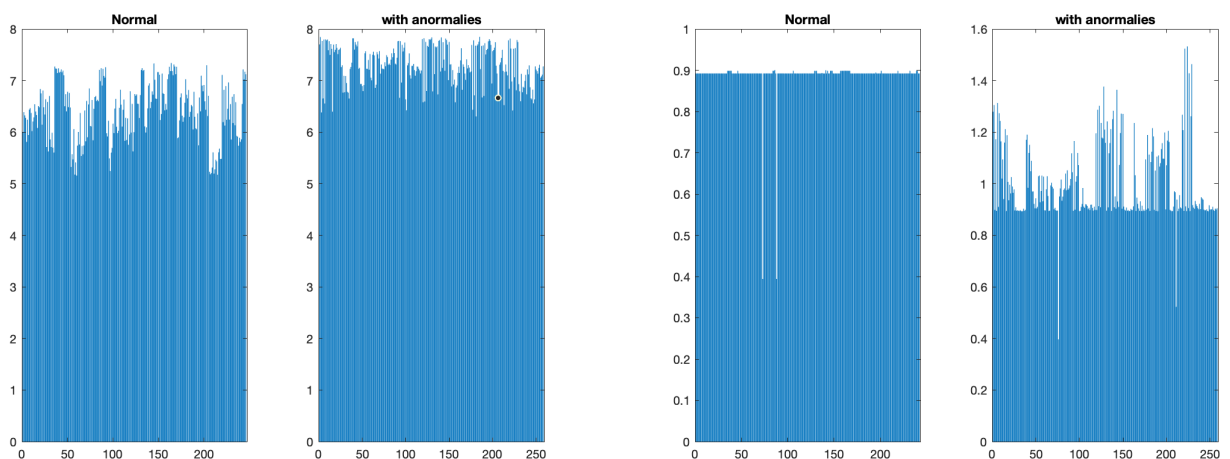


NORMAL DATA WAVELET RESULT

WAVELET RESULT OF DATA WITH ANOMALY

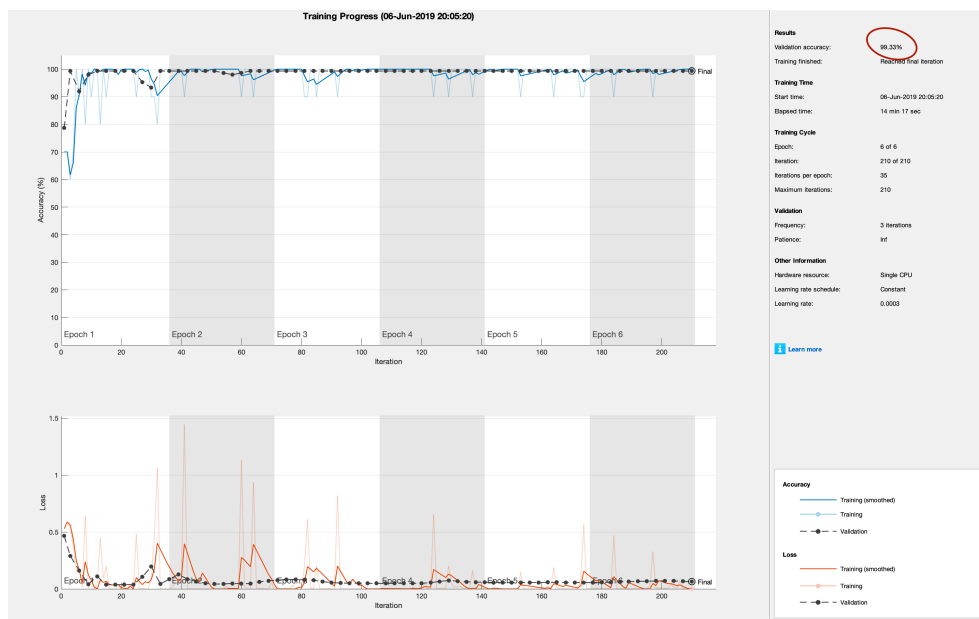
Comparing the two images, The difference between the two different data is clearer than looking directly at the radargrams.

To better analyze the even better, the entropy of the radargrams versus the wavelet transform results were calculated.

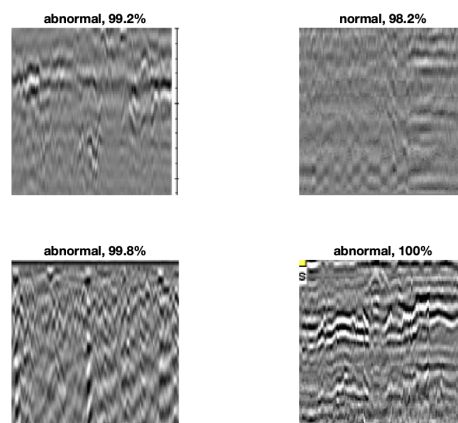


The differences in energy between the normal and the data with anomalies is much clearly when looking at the wavelet result entropy. This shows that using the wavelet results would provide a better classification result.

The Dataset fed to the CNN comprises of 258 wavelet transform images of data with anomalies and 242 wavelet transform images of normal data. The data was loaded into the same CNN as the lab experiment and the classification accuracy was calculated.



CNN classification result



Classification accuracy

It can be seen that the network gets better result for big scale data.

CHAPTER 5

CONCLUSION AND FUTURE WORK

Bridges, roads, tunnels, and other structures made of concrete are vital to the society and humans at large. Age, weather conditions, over-usage, and lack of proper maintenance cause these structures to wear and not reach their full lifespan potential. This can result in accidents, causing loss of lives and property.

New techniques are being developed to help check the health of these structures within a short period and saving costs. The Ground penetrating Radar (GPR) is one of the most common techniques.

Due to the complexity of the GPR Raw-Data, an unprofessional person would find it difficult to interpret and detect crack by just looking at the extracted images or signals. After the wavelet transform is done, it becomes easier to differentiate between a cracked and non-cracked data after using the complex wavelets. The entropy for the cracked vs. non-cracked data was calculated for the raw-data images and the wavelet results. After comparing the entropies, it was concluded that using the wavelet results is indeed better than using the raw-data to classify the data. Using CWT with complex wavelets is better than using DWT with normal wavelets. DWT is very similar to Fast Fourier transform. Because human beings are slow and prone to error, the neural network is used to classify the data as cracked or non-cracked more efficiently, showing the classification accuracy. The convolutional neural network was used because it is best for image classification.

The GPR Data from the lab experiments of this thesis were hard to interpret because the cracks were relatively small. Even for a professional, the cracks would be hard to detect from looking at the raw-data because the cracks were 2cm or smaller. The neural network validation and classification accuracy were low because of this. The work of this thesis is more successful for big cracks.

This thesis work was done on GPR to detect crack from its raw-data with the help of wavelets and neural networks. From the results gotten so far from this thesis, this is an effective method which can help this technique become more efficient and more user-friendly.

In the current experiment, the neural network was designed to classify the data as either cracked or not cracked or something similar.. For future studies, the goal will be to achieve a more complex classification like a difference in shapes, materials, etc.

REFERENCES

- F. Yiğit, G. Tucker, S. Özçelik. (2017). *GPR (Ground Penetrating Radar) Survey at Notion*. [online journal]. 978-1-5386-5777-5/18/\$31.00 ©2018 IEEE
- C. Wang, X. Liu.(2018) *Study of object recognition with GPR based on STFT*. [online journal]. GPR Engineering Department , China Research Institute of Radio Wave Propagation Qingdao, China. 978-1-5386-5777-5/18/\$31.00 ©2018 IEEE
- Smitha N.,(2017) *Wavelet based clutter reduction of GPR data*. In *Proceeding of Second International conference on Circuits, Controls and Communications*. 978-1-5386-0615-5/17/\$31.00 ©2017 IEEE
- Shreedhar S. T. Et al, (2017) *Detection of Debondings with Ground Penetrating Radar using a Machine Learning Method* .
- R. Ghozzi et al,(2017) *Peak detection of GPR data with Lifting Wavelet Transform (LWT)*. In *2017 International Conference on Advanced Systems and Electric Technologies*. 978-1-5090-6634-6/17/\$31.00 ©2017 IEEE
- M. M. Thakur, A. Prashant,(2016) *GPR Investigation at two sites of archeological interest in Vadnagar, India*. 2016 16th International conference of ground penetrating radar. 978-1-5090-5181-6/16/\$31.00 @2016 IEEE
- J. S. Kobashigawa, H.-S. Youn, M. F. Iskander, Z. Yun.,(2011) *Classification of buried targets using ground penetrating radar: comparison between genetic programming and neural networks*. IEEE ANTENNAS AND WIRELESS PROPAGATION LETTERS, VOL. 10, 2011. 1536-1225/\$26.00 © 2011 IEEE
- X. Wei, X. Chaoyang.,(2010) *Signal Filtering based on Wavelet Transform and Its Application in Ground Penetrating Radar*. 2010 international conference on communications and mobile computing. 978-0-7695-3989-8/10 \$26.00 © 2010 IEEE. DOI 10.1109/CMC.2010.210
- Z. Huasheng.(2009) *Study on Roadbed Disease Recognition Algorithm based on support vector machine*. 978-1-4244-3986-7/09/\$25.00 ©2009 IEEE
- E. Pasolli, F. Melgani, M. Donelli, R. Attoui, M. D. Vos.,(2008) *AUTOMATIC DETECTION AND CLASSIFICATION OF BURIED OBJECTS IN GPR IMAGES USING GENETIC ALGORITHMS AND SUPPORT VECTOR MACHINES*.

978-1-4244-2808-3/08/\$25.00 ©2008 IEEE

M. Yao, H. Wang, C. Wang,.(2007) *Target of Imaging Observation Based on The Wavelet Transform and GPR*. The 33rd Annual Conference of the IEEE Industrial Electronics Society (IECON) Nov. 5-8, 2007, Taipei, Taiwan. 1-4244-0783-4/07/\$20.00 (C)2007 IEEE

X. -L. CHEN, M. Tian, W. -B. Yao,.(2005) *GPR SIGNALS DE-NOISING BY USING WAVELET NETWORKS*. Proceedings of the Fourth International Conference on Machine Learning and Cybernetics, Guangzhou, 18-21 August 2005. 0-7803-9091-1/05/\$20.00 ©2005 IEEE

G. Kilic, L. Eren,.(2018) *Neural network based inspection of voids and karst conduits in hydro–electric power station tunnels using GPR*. Journal of Applied Geophysics 151 194–204. <https://doi.org/10.1016/j.jappgeo.2018.02.026>. 0926-9851/ © 2018 Elsevier B.V.

M. Almainani.(2018). *CLASSIFYING GPR IMAGES USING CONVOLUTIONAL NEURAL NETWORKS*. Master's Thesis. University of Tennessee at Chattanooga. Department of Computer Science. 51 p.

Developers, GeoSci.xyz.(2015) *Ground Penetrating Radar. Ground Penetrating Radar - Electromagnetic Geophysics*, em.geosci.xyz/content/geophysical_surveys/gpr/index.html.

Kilic, G. (2016) *Applications of Ground-Penetrating Radar (GPR) to Detect Hidden Beam Positions*. Journal of Testing and Evaluation, doi:10.1520/JTE20150325. ISSN 0090-3973

Kilic, G. and Unluturk, M. S.,(2016) *GPR Raw-Data Analysis to Detect Crack Using Order Statistic Filtering*. Journal of Testing and Evaluation, doi:10.1520/JTE20150057. ISSN 0090- 3973

Kilic, G.(2014) *GPR Raw-Data Order Statistic Filtering and Split-Spectrum Processing to Detect Moisture*. Remote Sens. 2014, 6, 4687-4704; doi:10.3390/rs6064687

Kilic, G., Unluturk, M. S, (2014). *Performance evaluation of the neural networks for moisture detection using GPR, Nondestructive Testing and Evaluation*. DOI: 10.1080/10589759.2014.941839

Lee E.J., Shin S.Y., Ko B.C., Chang C. (2016) *Early sinkhole detection using a drone-based thermal camera and image processing*. Infrared Physics & Technology, ISSN: 1350-4495, Vol: 78, Page: 223-232, DOI: [10.1016/j.proeng.2017.02.164](https://doi.org/10.1016/j.proeng.2017.02.164)

A. Szajewska (2017) . *Development of the Thermal Imaging Camera (TIC) Technology*. Procedia Engineering, ISSN: 1877-7058, Vol: 172, Page: 1067-1072, DOI: [10.1016/j.proeng.2017.02.164](https://doi.org/10.1016/j.proeng.2017.02.164)

Mohammed A. Isa; Ismail Lazoglu (2017). *Design and analysis of a 3D laser scanner*. Measurement, ISSN: 0263-2241, Vol: 111, Page: 122-133. DOI: [10.1016/j.measurement.2017.07.028](https://doi.org/10.1016/j.measurement.2017.07.028)

Graps, Amara. (1995). *An Introduction to Wavelets*. IEEE Comp. Sci. Engi.. 2. 50-61. 10.1109/99.388960.

Ivan Nunes da Silva et al.,(2017) *Artificial Neural Networks A Practical Course*. DOI: [10.1007/978-3-319-43162-8](https://doi.org/10.1007/978-3-319-43162-8)

Addison, P. S. (2017). *The illustrated wavelet transform handbook: introductory theory and applications in science, engineering, medicine and finance*. CRC press.

APPENDIX 1 – CWT with Matlab

```
clear all
close all
direc = "/users/thegang/Desktop/LabData/DatFiles";
sc=0.1:0.1:4;

list=dir('*.dat');

for i=1:length(list)
    filename = list(i).name;
    M = csvread(filename,1,0);
    ctemp=abs(cwt(M(:,2),sc,'cmor1-10')); % Cmor 1 to 10
    ctemp=imresize(ctemp,[224 224]);
    im = ind2rgb(im2uint8(rescale(ctemp)),jet(128));
    cd data
    imname=strcat(num2str(i),'.png');
    imwrite(im,imname,'png')
    cd ..
end
```

APPENDIX 2 – Calculating entropy in Matlab

```
%%  
  
clear all  
  
close all  
  
list=dir('users/thegang/Documents/MATLAB/LabData/  
targets\nocrack\*CM120.png');  
  
for i=3:length(list)  
    A=imread(list(i).name);  
    A=rgb2gray(A);  
    ent(i-2)=entropy(A);  
  
end  
  
%%  
  
list1=dir('users/thegang/Documents/MATLAB/LabData/  
targets\cracked\*CM120.png');  
  
cd('users/thegang/Documents/MATLAB/LabData/targets\cracked\  
)  
  
for i=3:length(list1)  
    A=imread(list1(i).name);  
    A=rgb2gray(A);  
    entc(i-2)=entropy(A);  
  
end  
  
figure,  
subplot(121),bar(ent),title('No-Crack')  
subplot(122), bar(entc),title('Crack')
```


APPENDIX 3 – Training CNN to classify new image

```
path_data = "/users/thegang/Documents/MATLAB/LabData/targets";
imds = imageDatastore(path_data, ...
    'IncludeSubfolders',true, ...
    'LabelSource','foldernames');
[imdsTrain,imdsValidation] = splitEachLabel(imds,0.7);
net = googlenet;
analyzeNetwork(net)
net.Layers(1)
inputSize = net.Layers(1).InputSize;
if isa(net,'SeriesNetwork')
    lgraph = layerGraph(net.Layers);
else
    lgraph = layerGraph(net);
end
[learnableLayer,classLayer] = findLayersToReplace(lgraph);
[learnableLayer,classLayer]
numClasses = numel(categories(imdsTrain.Labels));
if isa(learnableLayer,'nnet.cnn.layer.FullyConnectedLayer')
    newLearnableLayer = fullyConnectedLayer(numClasses, ...
        'Name','new_fc', ...
        'WeightLearnRateFactor',10, ...
        'BiasLearnRateFactor',10);
elseif isa(learnableLayer,'nnet.cnn.layer.Convolution2DLayer')
    newLearnableLayer = convolution2dLayer(1,numClasses, ...
        'Name','new_conv', ...
        'WeightLearnRateFactor',10, ...
        'BiasLearnRateFactor',10);
end
lgraph = replaceLayer(lgraph,learnableLayer.Name,newLearnableLayer);
```

```

newClassLayer = classificationLayer('Name','new_classoutput');
lgraph = replaceLayer(lgraph,classLayer.Name,newClassLayer);
figure('Units','normalized','Position',[0.3 0.3 0.4 0.4]);
plot(lgraph)
ylim([0,10])
options = trainingOptions('sgdm', ...
    'MiniBatchSize',10, ...
    'MaxEpochs',6, ...
    'InitialLearnRate',3e-4, ...
    'Shuffle','every-epoch', ...
    'ValidationData',imdsValidation, ...
    'ValidationFrequency',3, ...
    'Verbose',false, ...
    'Plots','training-progress');
net = trainNetwork(imdsTrain,lgraph,options);
[YPred,probs] = classify(net,imdsValidation);
accuracy = mean(YPred == imdsValidation.Labels)
idx = randperm(numel(imdsValidation.Files),4);
figure
for i = 1:4
    subplot(2,2,i)
    I = readimage(imdsValidation,idx(i));
    imshow(I)
    label = YPred(idx(i));
    title(string(label) + ", " + num2str(100*max(probs(idx(i),:)),3)
+ "%");
end

```

APPENDIX 4 – Single-Level 2-D Discrete Wavelet Transform of an Image with Matlab

```
% Load and display an image.

xi = imread("/users/thegang/Documents/MATLAB/LabData/targets/
Radargrams/normal/B52.png");

figure ; imshow(xi);

imagesc(xi)

colormap(map)

%%

% Obtain the single-level 2-D discrete wavelet transform of the
image using

% the order 10 Daubechies and periodic extension.

[cA,cH,cV,cD] = dwt2(xi,'db10','mode','per');

%%

% Display the vertical detail coefficients and the approximation
coefficients.

imagesc(cV)

title('Vertical Detail Coefficients')

imagesc(cA)

title('Approximation Coefficients')
```

APPENDIX 5 – Resizing image to 224

```
clear all
close all
cd normal
list=dir('*.*png');
for i=1:length(list)
    filename = list(i).name;
    c=imread(filename);
    for j=1:3
        ctemp(:,:,j)=imresize(c(:,:,j),[224 224]);
    end
    imwrite(ctemp,filename,'png')
    clear ctemp
    clear c
end
```